

HUMAN GAIT MODELLING AND ANALYSIS

CHAN YU T'NG

**A project report submitted in partial fulfilment of the
requirements for the award of Bachelor of Engineering
(Honours) Biomedical Engineering**

**Lee Kong Chian Faculty of Engineering and Science
Universiti Tunku Abdul Rahman**

April 2020

DECLARATION

I hereby declare that this project report is based on my original work except for citations and quotations which have been duly acknowledged. I also declare that it has not been previously and concurrently submitted for any other degree or award at UTAR or other institutions.

Signature : 

Name : Chan Yu T'ng

ID No. : 15UEB01920

Date : 24th April 2020

APPROVAL FOR SUBMISSION

I certify that this project report entitled “**HUMAN GAIT MODELLING AND ANALYSIS**” was prepared by **CHAN YU T’NG** has met the required standard for submission in partial fulfilment of the requirements for the award of Bachelor of Engineering (Honours) Biomedical Engineering at Universiti Tunku Abdul Rahman.

Approved by,

Signature

:



Supervisor

:

Dr. Chan Siow Cheng

Date

:

24th April 2020

Signature

:



Co-Supervisor

:

Mr. Chong Yu Zheng

Date

:

24th April 2020

The copyright of this report belongs to the author under the terms of the copyright Act 1987 as qualified by Intellectual Property Policy of Universiti Tunku Abdul Rahman. Due acknowledgement shall always be made of the use of any material contained in, or derived from, this report.

© 2020, Chan Yu T'ng. All right reserved.

ABSTRACT

The goal of this research is to develop a simple and cost-effective gait analysis system to compute the joint moments of lower extremities in the sagittal plane with available tools and software. The proposed gait analysis system involves three devices which are a digital camera, a split-belt instrumented treadmill (H/P Cosmos™ Instrumented Treadmill) and a personal computer equipped with Gaitway software and SkillSpector software. The digital camera and SkillSpector software were used as a motion capture system to acquire the trajectories of the markers and perform kinematic analysis to obtain linear and angular kinematic parameters. The coordinates of the markers obtained from SkillSpector together with the force data obtained from the treadmill and Gaitway software were then used as input to perform inverse dynamics analysis to obtain joint moment in the Microsoft Excel spread sheet. Two subjects (one male and one female) were recruited to test the system and the outputs of the system were then validated against existing data. In overall, the system produces reliable kinematic and kinetic results comparable to those experimental results.

TABLE OF CONTENTS

TABLE OF CONTENTS		i
LIST OF TABLES		iii
LIST OF FIGURES		iv
LIST OF SYMBOLS / ABBREVIATIONS		vii
LIST OF APPENDICES		viii
 CHAPTER		
1	INTRODUCTION	1
	1.1 General Introduction	1
	1.2 Importance of the Study	2
	1.3 Problem Statement	2
	1.4 Aim and Objectives	2
	1.5 Scope and Limitation of the Study	3
2	LITERATURE REVIEW	5
	2.1 Introduction	5
	2.2 Literature Review	5
	2.2.1 Comparison of Available Software System	5
	2.2.2 Inverse Dynamics Model	7
	2.2.3 Software – SkillSpector	9
	2.2.4 Marker Placement for two-dimensional gait analysis	11
	2.3 Summary	12
3	METHODOLOGY AND WORK PLAN	13
	3.1 Introduction	13
	3.2 Data Acquisition	14
	3.3 Data Analysis	15
	3.3.1 Kinematic Analysis	15
	3.3.2 Kinetic Analysis	19
	3.3.3 Statistical Analysis	24
4	RESULTS AND DISCUSSIONS	25

4.1	Introduction	25
4.2	Data Validation	25
4.2.1	Kinematic Parameters	25
4.2.2	Kinetic Parameters	31
4.3	Factors Affecting Magnitude of Kinematic and Kinetic Data	38
4.4	Difference between CoM and CoP	39
4.5	Summary	40
5	CONCLUSIONS AND RECOMMENDATIONS	41
5.1	Conclusions	41
5.2	Recommendation for future work	41
	REFERENCES	43
	APPENDICES	51

LIST OF TABLES

TABLE	TITLE	PAGE
2.1	Summary of Analysis of Different Software Systems.	7
3.1	Anthropometric Parameter Estimation.	21
3.2	Assumptions Made on Location of CoP.	23
4.1	Peak Values of Ankle Joint Angle.	28
4.2	Peak Values of Knee Joint Angle.	31
4.3	Peak Values of Ankle Joint Moment.	34
4.4	Peak Values of Knee Joint Moment.	37

LIST OF FIGURES

FIGURE	TITLE	PAGE
1.1	Anteroposterior, Vertical and Mediolateral Components of Ground Reaction Force (Watkins, 2010).	4
2.1	Anatomical Model and Link Segment Model.	8
2.2	2D Model Marker Placement (Hickox, 2014).	11
3.1	The Flowchart of Methodology.	13
3.2	Marker Placement.	14
3.3	Top View of Setup for Data Acquisition.	14
3.4	Defining Number of Points to be Digitized.	16
3.5	Assigning Point Names.	16
3.6	Defining Segments.	16
3.7	Defining Calibration Points.	17
3.8	Digitizing Movement.	17
3.9	Digitizing Calibration.	17
3.10	Setting Filtering Parameters.	18
3.11	Output of SkillSpector.	19
3.12	2D Sagittal Plane FBD (Kirtley, 2006).	21
4.1	FBD for Measurement of Ankle Joint Angle (Perry and Davids, 1992).	26
4.2	The Graph of Ankle Joint Angle against Percentage of Gait Plotted from Analysis for Female Subject.	26
4.3	The Graph of Ankle Joint Angle against Percentage of Gait Plotted from Analysis for Male Subject.	26

4.4	(a) Ankle Range of Motion for a Gait Cycle (Perry and Davids, 1992). (b) Ankle Joint Angle Measured using Electrogoniometer against Percentage of Gait in Sagittal Plane (Moriguchi, Sato and Gil Coury, 2007). (c) Sagittal Plane Ankle Joint Angle. IC = Initial Contact; HR = Heel Rise; TO = Toe Off (Musculoskeletal Key, 2016).	27
4.5	FBD for Measurement of Knee Joint Absolute Angle (Perry and Davids, 1992).	29
4.6	The Graph of Knee Joint Angle against Percentage of Gait Plotted from Analysis for Female Subject.	29
4.7	The Graph of Knee Joint Angle against Percentage of Gait Plotted from Analysis for Male Subject.	29
4.8	(a) Knee Range of Motion for a Gait Cycle (Perry and Davids, 1992). (b) Changes in Angle of Knee Flexion during Linear Walking (Qiu, et al., 2017). (c) Sagittal Plane Knee Joint Angle (Musculoskeletal Key, 2016).	30
4.9	Convention for Ankle Joint Moment.	32
4.10	The Graph of Ankle Joint Moment against Percentage of Gait Plotted from Analysis for Female Subject.	32
4.11	The Graph of Ankle Joint Moment against Percentage of Gait Plotted from Analysis for Male Subject.	32
4.12	(a) Sagittal Plane Internal Joint Moments of Ankle during Walking (Sobhani, Dekker, Postema and Dijkstra, 2012). (b) Sagittal Plane Ankle Moments from Gait Analysis of Five Walking Trials (Brockett and Chapman, 2016). (c) Sagittal Plane Ankle Joint mMoment (Musculoskeletal Key, 2016).	33
4.13	Convention for Knee Joint Moment.	35
4.14	The Graph of Knee Joint Moment against Percentage of Gait Plotted from Analysis for Female Subject.	35

4.15	The Graph of Knee Joint Moment against Percentage of Gait Plotted from Analysis for Male Subject.	35
4.16	(a) Sagittal Plane Internal Joint Moments of Knee during Walking (Sobhani, Dekker, Postema and Dijkstra, 2012). (b) Moment at the Knee during the Gait Cycle (Winter, 1987). (c) Sagittal Plane Knee Joint Moment (Musculoskeletal Key, 2016).	36
4.17	Record of CoM and CoP in Anterior Posterior Direction during Erect Standing (Winter, 2009).	39
4.18	The Graph of Ankle Joint Moment against Percentage of Gait Plotted from Analysis for Female Subject when CoM is Misinterpreted as CoP (Red Line).	40

LIST OF SYMBOLS / ABBREVIATIONS

F	force, N
m	mass, kg
a	acceleration, m/s^2
M	moment, $\text{N}\cdot\text{m}$
I	mass moment of inertia, $\text{kg}\cdot\text{m}^2$
α	angular acceleration, rad/s^2
g	gravitational force, m/s^2
p	proximal joint
d	distal joint
ρ	radius of gyration, m
F_x	anteroposterior ground reaction force
F_y	vertical ground reaction force
F_z	mediolateral ground reaction force
VGRF	vertical ground reaction force
EMG	electromyography
2D	two-dimensional
3D	three-dimensional
CoM	centre of mass
CoP	centre of pressure
DLT	direct linear transformation
ISB	International Society of Biomechanics
MTP5	fifth metatarsophalangeal
FBD	free body diagram

LIST OF APPENDICES

APPENDIX A: Graphs	51
A-1 The Graph of VGRF against Gait Cycle for Female Subject.	51
A-2 The Graph of VGRF against Gait Cycle for Male Subject.	51

CHAPTER 1

INTRODUCTION

1.1 General Introduction

Human gait is a pattern of locomotion associated with their posture, and gait analysis refers to research related to human walking. It is a way to disclose how human walk by evaluating factors that controls the performance of the lower extremities.

Gait studies have two main tracks: clinical gait analysis and biometric goal of human gait analysis. Clinical gait analysis depends on data acquisition in controlled environment (Katiyar, Pathak and Kumar, 2010) while biometric goal of human gait analysis performs data acquisition in different areas and scenario (Nandy, et al., 2014). Clinical gait analysis includes five elements: videotape examination, temporal-spatial analysis, kinematic analysis, kinetic analysis and electromyography (Fandaklı, Okumuş and Öztürk, 2018). Temporal-spatial analysis identifies the parameters such as step length, stride length, cadence, walking speed etc. Kinematic analysis describes the motion of the joints in the lower limb without any reference to forces (Nikravesh, 1988) and kinetic analysis determines the power and moment exerted by the joints while walking (Pfister, et al., 2014).

In recent years, numerous gait models have been developed to study the behaviour of human locomotion. The major reason behind this development is due to the possibility of quantitative prediction, hypothesis testing and estimation of dynamic parameters such as forces and moments of the joints that are not directly measurable (Siegler, Selikta and Hyman, 1982). These models are being widely used in different application such as biomechanics research, ergonomics, sport biomechanics, medical device design and orthopaedics (Liu, et al., 2008; Thomas, et al., 2014; Debaere, et al., 2015; Abad, et al., 2018; Fandaklı, Okumuş and Öztürk, 2018).

1.2 Importance of the Study

Joint forces and moments are important parameters commonly used in gait analysis for biomechanics research, ergonomics, sport biomechanics, medical device design or orthopaedics. The system proposed in this research aims to provide reliable quantitative kinematics and kinetic information of human gait using simple and affordable tools. The proposed system can assist in future research in better understanding of the experimental subject's gait pathology and the activity occurred at the joint during gait.

1.3 Problem Statement

In order to monitor and analyse gait movement in detail, assistance of software systems is required as some parameters such as forces and moments of the joints that are not directly measurable. Software systems that allows biomechanics researchers to create own models and perform analyses is widely available nowadays. However, most of the source code of available software is not accessible by public (Delp, et al., 2007) and users need to purchase the complete code in order to perform biomedical analysis. In addition, most of the software systems available require certain level of technical expertise to operate, controlled environment and expensive tools such as motion capture systems to obtain the input parameters. In response to this problem, this research aims to propose a simple way of performing gait analysis on the lower limb with available or affordable tools.

1.4 Aim and Objectives

This project aims to propose a simple and cost-effective gait analysis system with available tools and software.

The specific objectives of this project include:

1. Build a human kinematic model to compute the joint moments of lower extremities using available software.
2. Validate the modelling results with existing experimental data.

1.5 Scope and Limitation of the Study

This study mainly focuses on performing gait analysis on sagittal plane of lower limb using a single digital camera together with a treadmill (H/P Cosmos™ Instrumented Treadmill).

Motion capture activity is required to be carried out at a large empty room equipped with six or more motion capture cameras to capture the motion of the subject in three-dimensional (3D). However, due to limitation of resources, it is not realistic. Furthermore, the motion capture analysis software is costly. Hence, this study proposed to use a video captured by a single digital camera from the sagittal plane for analysis of human movement. Although analysis performed in sagittal plane may cause loss of movement characteristics in other planes (Umberger and Martin, 2001), it does provide an easy way to obtain a valid data with lower cost. Kinetic analysis in sagittal plane can be a useful tool to perform gait analysis (Olney, et al., 1991).

In order to perform inverse dynamics to determine joint moment, 3D inputs from the force platform are required. However, the treadmill that was used can only provide two-dimensional (2D) data which is the vertical ground reaction force (VGRF). Hence, in the calculation of joint reaction force and joint moment, only VGRF was considered while the horizontal ground reaction force was not taken into consideration. Horizontal ground reaction force is the shear forces acting on the surface of platform and can be classified into the anteroposterior (F_x) and mediolateral (F_z) ground reaction force, where anteroposterior is the shear force acting on the toe-heel axis while mediolateral force is the shear force acting on left-right axis of the foot. Mediolateral force is small when walking straight forward due to very little side-to-side movement of body (Watkins, 2010).

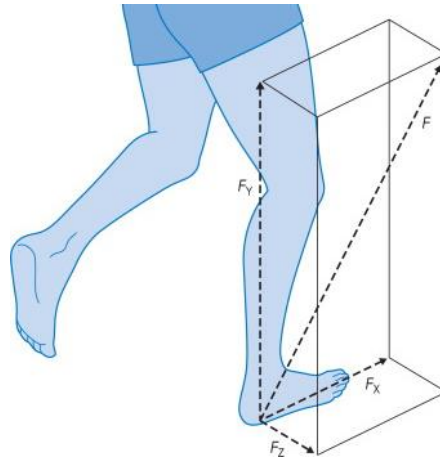


Figure 1.1: Anteroposterior, Vertical and Mediolateral Components of Ground Reaction Force (Watkins, 2010).

In addition, few assumptions were being made while adopting the inverse dynamics technique. First of all, friction caused by the split-belt is assumed to be zero. Friction at the joint is also assumed to be negligible; the resultant bone-to-bone contact forces are very close to the geometrical axis of the and hence its contribution to net moment is assumed to be negligible (Camomilla, et al., 2017). Next, the anthropometric parameters are estimations and are generalized, this approach neglects the contribution of gravitational forces and segment inertial, assuming the mass distribution in a segment is concentrated at one point. Since the anthropometric parameters are generalized, the model may not work well with under or overweight subjects, children and patients with wasted legs.

Furthermore, the moment obtained from inverse dynamics can only indicate which muscle (flexor or extensor) was active, and moment exerted by that muscle, it cannot distinguish between different muscles. In order to study each muscle, electromyography (EMG) is required. Hence, due to limitation of resources, the study of muscles was not carried out.

CHAPTER 2

LITERATURE REVIEW

2.1 Introduction

With given range of human motion related locomotion, many relevant techniques and software have been developed to perform human gait modelling and analysis. This part of the report discusses about the previous research done on human gait modelling and analysis with techniques and software available by comparing their specifications and capabilities.

2.2 Literature Review

2.2.1 Comparison of Available Software System

Software-based motion analysis plays an important role in assess motion or movement in a quicker and more reliable way. In order to achieve this, motion data needs to be processed, and maps the tracked information to motion description (Nunes, Moreira and Tavares, 2016).

The earliest musculoskeletal modelling software is known as SIMM (Software for Interactive Musculoskeletal Modelling), developed by MusculoGraphics, Inc. (USA). This software system allows researchers to perform movement analysis on upper and lower extremities (Holzbaur, Murray and Delp, 2005; Bachynskyi, et al., 2014). Over the years, numerous software systems such as AnyBody, Kinovea, MSMS, OpenSim, SIMM, SkillSpector and Visual3D that offer the capability to perform modelling and analysis gradually emerge in the market.

AnyBody Modeling System tool available at AnyBody Technology was initially developed at Aalborg University. This software is capable to perform 3D analysis and stimulation of human movement interacting with environment (Bajelan and Azghani, 2014). On the other hand, Visual3D is a tool used for managing, modelling, stimulating and analysing motion data in 2D or 3D (Noehren, et al., 2014). However, similar to SIMM, these two software systems are not freely available, users need to purchase the full code in order to install and perform any analysis.

MSMS (Musculoskeletal Modelling Software) developed at the University of South California is a software that allows motion modelling, simulations and analysis of neural prostheses systems in 3D (Chauhan and Vyas, 2013), although it is freely available, it does not provide a complete source code to public causes biomechanics researches difficult to improve their capabilities (Delp, et al., 2007). Opensim developed by Delp, et al. (2007) provides a freely available, open source platform allowing users to acquire human models to perform simulation and analysis in 3D. It also allows users to write their own plug-ins for control or analysis. Similar to the four software systems mentioned above, input of Opensim requires motion data to be obtained from a 3D motion capture system.

Kinovea is a video-based movement analysis software that allows user to measure distances and times to follow the trajectories of points (Hisham, et al., 2017). The major drawback of this software is that only kinematics parameters can be obtained from this software. Another alternative to Kinovea is the SkillSpector software developed by Video4coach. This software allows user to perform offline motion tracking and analysis in 2D or 3D with digital camera. The main difference between Kinovea and SkillSpector is that SkillSpector is able to provide more possibilities for movement analysis (Omorczyk, et al., 2014), it is able to provide limited kinetic analysis such as potential and kinetic energy.

The summary of analysis software systems discussed above was tabulated in Table 2.1.

Table 2.1: Summary of Analysis of Different Software Systems.

Software	Availability	Analysis	Simulations	Inputs requirement
AnyBody	Commercial	3D	3D	Motion data, EMG, Force data
Kinovea	Free	2D	NA	Video
MSMS	Free	3D	3D	Motion data, EMG
OpenSim	Free	3D	3D	Motion data, EMG, Force data
SIMM	Commercial	2D or 3D	3D	Motion data, EMG, Force data
SkillSpector	Free	2D or 3D	NA	Video
Visual3D	Commercial	3D	2D or 3D	Motion data, EMG, Force data

2.2.2 Inverse Dynamics Model

Inverse dynamics involves working back from the kinematic data to derive the kinetic output for motion. It is a commonly used method to estimate joint moments and forces based on extremity movement, anthropometric parameters and ground reaction force. The procedure of inverse dynamics starts with measuring ground reaction force, beginning with the segments that are in contact to the ground, the joint forces and moments of each successive segment were calculated (Vaughan, Davis and O'connor, 1992; Siegler and Liu, 1997). Inverse dynamics models are not only useful for walking gait analysis, it is also useful in assessing other complex movements such as load carriage (Ren, Jones and Howard, 2005) and balance controls (Robert et al., 2007).

In inverse dynamics, a link-segment model is defined. A link-segment model is a model that replaces joints with hinge joints and segments with masses and moments of inertia about the centre of mass (CoM). The forces that are acting on the link-segment model include gravitational force, external force (e.g. ground reaction force), muscle and ligament force, and joint reaction force. The model can be described using the classical Newton-Euler equations (Equation 2.1 and Equation 2.2).

$$\text{Newton (linear): } F = ma \quad (2.1)$$

$$\text{Euler (angular): } M = I\alpha \quad (2.2)$$

where

F = force, N

m = mass, kg

a = acceleration, m/s^2

M = moment, $\text{N}\cdot\text{m}$

I = mass moment of inertia, $\text{kg}\cdot\text{m}^2$

α = angular acceleration, rad/s^2

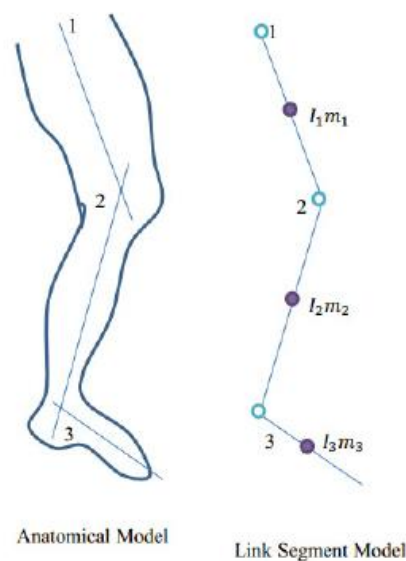


Figure 2.1: Anatomical Model and Link Segment Model.

The inputs of inverse dynamics are divided into three categories: anthropometric information, kinematic information and kinetic information. Each type of inputs is error-prone and uncertain, being kinematic input the most sensitive. For instance, a misconception of body segments or a disturbance in the application point will strongly affect the quality of result (Silva and Ambrósio, 2004).

Inverse dynamics were performed on both Newington and Helen Hayes model to predict the joint moments. Newington group perform inverse dynamics with anthropometric parameters from Dempster's work (Dempster, 1955; Dempster, Gabel and Felts, 1959), on the other hand Helen Hayes group

performed inverse dynamics with anthropometric parameters from Hinrichs's work (Hinrichs, 1985). The output of both analysis giving similar results, showing that joint moments are insensitive to anthropometric parameters (Pearsall and Costigan, 1999; Rao, et al., 2006).

Alkjaer, Simonsen and Dyhre-Poulsen (2001) carried out a research to compare the 2D and a 3D inverse dynamics model. It was found that although differences were observed in the magnitude of joint moments, the overall time course pattern of joint moments were almost identical in 2D and 3D. They concluded that the simpler 2D sagittal plane model is appropriate for human gait analysis. Ren, Jones and Howard (2008) further reported that inverse dynamics performed in the sagittal plane were more accurate compared to other planes due to larger magnitudes in sagittal plane in comparison with the other planes. Various researches have also proposed numerous techniques to assess lower limb motion in the sagittal plane and suggest that analysis carried out at the sagittal plane is capable generating highly reliable data with normal healthy subjects (Ugbolue, et al., 2013; Castelli, et al., 2015).

2.2.3 Software – SkillSpector

SkillSpector is freely available and user friendly software developed by Video4coach that provides a simple and practical way of performing offline motion tracking and analysis in 2D or 3D. SkillSpector is also capable to combine all video, kinematics data and animation of the movement in one complete analysis and the progression of the kinematic data and animation can be visualized by navigating in the video.

In SkillSpector, human body was simplified into model consist of body points (i.e. toe, ankle, knee etc.) linked together by body segments (foot, shank, thigh etc.). The analysis of SkillSpector uses Direct Linear Transformation (DLT) algorithm to calculate the body position from a calibration object with known size and dimension. From the information of movement of body position in every frame, the software is able to calculate kinematic information such as linear and angular velocity, accelerations etc.

SkillSpector software was used by many researchers to perform kinematic analysis; Silvestre, et al. (2019) to determine kinematic parameters in the study of analysing changes in gait when weights are used in lower limbs;

Chagas, et al. (2013) to determine kinematic parameters of gait of Brazilian children; Nemtsev and Nemtseva (2017) to compare kinematics parameters of athletes' movement at the resistance and release instances of sprint running at maximum speed; Mirmoezzi, et al. (2015) to obtain kinematic data of free throws and jump shot; Nemtsev, et al. (2015) to perform 2D evaluation on take-off characteristics in long jump.

Furthermore, SkillSpector is also able to perform limited kinetic analysis. Hirunrat and Ingkatecha (2015) performed kinematics and kinetic analysis on jumping serve of volleyball players in Thailand with SkillSpector. The kinetic parameters selected were potential and kinetic energy during ball contact.

Omorczyk, et al. (2014) used Kinovea software in assessing artistic gymnastics technique carried out by a champion class artistic gymnast, and SkillSpector software was used to perform frame by frame video analysis to validate the result from Kinovea software and perform kinematic analysis. They found that same result can be generated from Kinovea and SkillSpector software although SkillSpector software is more complex, but it is able to perform more kinematic analysis.

Various researches have also used SkillSpector as a low-cost motion capture system to obtain trajectories of the markers attached on the subject. Abass and Faihan (2015) used SkillSpector software to obtain the 2D sagittal plane trajectories of reflective markers, the marker data were then used in MATLAB software to perform inverse dynamics and obtain Pedotti diagram for normal and abnormal subject. Similar to Abass and Faihan's (2015) work, Hamandi, Azzawi and Abdulwahed (2018) performed gait analysis with inverse dynamics in MATLAB software with marker data obtained from SkillSpector for patients that underwent a total hip replacement surgery. Karsai, Conceição and Takács (2019) analysed the reliability 3D underwater motion analysis system using three pieces of SJ4000 sports camera and SkillSpector software. The data series obtained from SkillSpector was exported to Microsoft Excel for further analysis. The result of this study showed that the system was suitable for practical 3D analysis of swimmer underwater.

2.2.4 Marker Placement for two-dimensional gait analysis

A 2D and 3D full body kinematics marker set were developed by Hickox (2014). The 3D model marker set was designed with reference of Ren, et al.'s (2008) work and recommendation by the International Society of Biomechanics (ISB) while the 2D model marker set was developed to match as closely as possible with the 3D model. The 2D link segment model developed by Hickox (2014) consists of seven segments linked together by eight markers located at the fifth metatarsophalangeal (MTP5), ankle, knee, hip, lower back, shoulder, elbow and wrist, as illustrated in Figure 2.2.

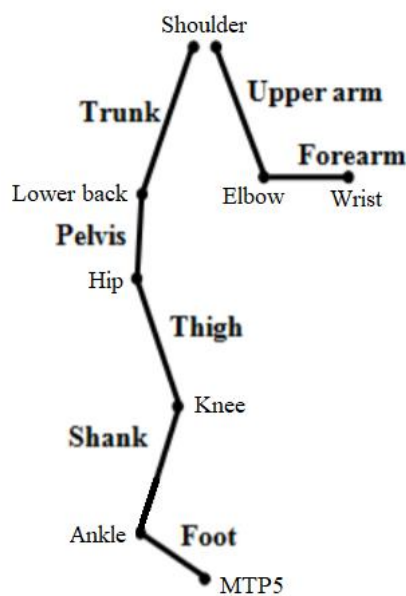


Figure 2.2: 2D Model Marker Placement (Hickox, 2014).

The inverse dynamics results of the study shows that the 2D and 3D methods in lower extremities were almost similar, proving the validity of the 2D model.

2.3 Summary

In this part of the report, human gait modelling and analysis research has been briefly reviewed and summarized as follow:

1. Software-based motion analysis plays a crucial role in increasing speed and reliability of motion analysis. Therefore, research has been carried out to select the most suitable software taking into considerations of availability of resources and research interest. SkillSpector software was selected.
2. The fact that SkillSpector software have been used by many other researches to perform kinematic analysis and used as a low-cost motion capture system have proven its reliability. Since SkillSpector software is not capable to calculate joint moments, Microsoft Excel will be incorporated to perform inverse dynamics.
3. Inverse dynamics is a popular approach to calculate joint moments. Previous researches done with inverse dynamics models were studied and the reliability of performing inverse dynamic in 2D sagittal plane and the insensitivity of different set of anthropometric parameters were confirmed. However, it was clearly stated that error in determining the kinematic information will strong affect the result, hence extra care must be taken while processing the kinematic input.
4. The marker placement of a 2D model was also studied. Since this project only focus on lower extremities, therefore only markers located at MTP5, ankle joint, knee joint and hip joint will be used in performing lower extremities kinematic and kinetic analysis.

CHAPTER 3

METHODOLOGY AND WORK PLAN

3.1 Introduction

Two young (between age of 20 to 25) and healthy subjects were recruited in the experiment. One female subject (height of 163 cm and mass of 49.0 kg) and one male subject (height of 170 cm and mass of 58.3 kg). In order to perform inverse dynamic analysis, kinematic and kinetic data of the subject must be gathered. Kinematic data acquisition was done by using simple arrangement which consists of a digital camera, sticker markers and a computer equipped with SkillSpector software. On the other hand, the kinetic data were obtained using treadmill (H/P Cosmos™ Instrumented Treadmill) and a personal computer equipped with Gaitway software which records VGRF acting on the feet. SkillSpector software and Microsoft Excel were then used to perform the analysis of gait parameters.

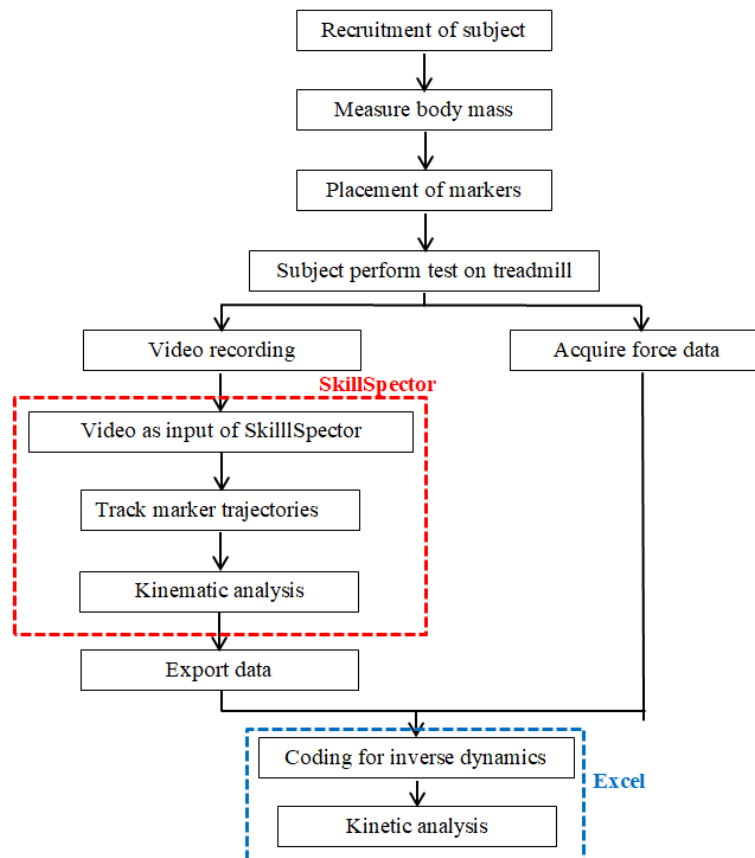


Figure 3.1: The Flowchart of Methodology.

3.2 Data Acquisition

Before the experiment, the weight of subjects was measured by the force plate embedded in the treadmill. Then, the coordinate of MTP5, ankle joint, knee joint and hip joint were marked by using four sticker markers, as shown in Figure 3.2. After the placement of the markers, the subject was instructed to walk at his or her own preferable speed (2.5 km/h for female subject 3.2 km/h for male subject) on the treadmill with a belt surface 0.5 m wide and 1.50 m long for 30 seconds. The paths of the markers were then recorded through a digital camera located at a distance of 1.0 m away from the treadmill providing a sagittal view of the subject, as illustrated in Figure 3.3. At the same time, the force data were acquired using the Gaitway software. After the collection of data, the data were then exported to perform analysis.

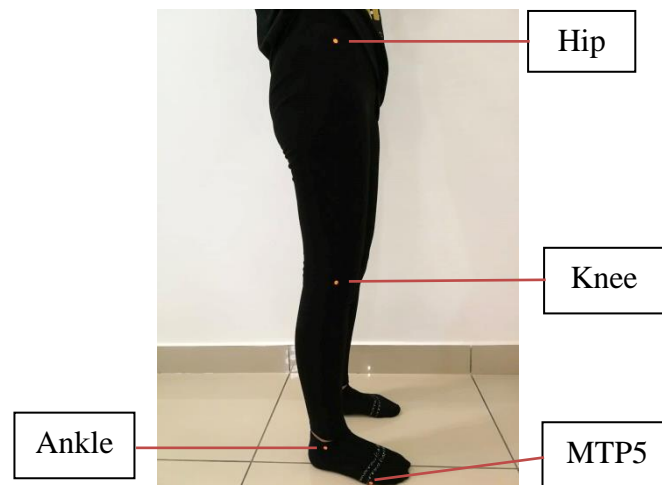


Figure 3.2: Marker Placement.

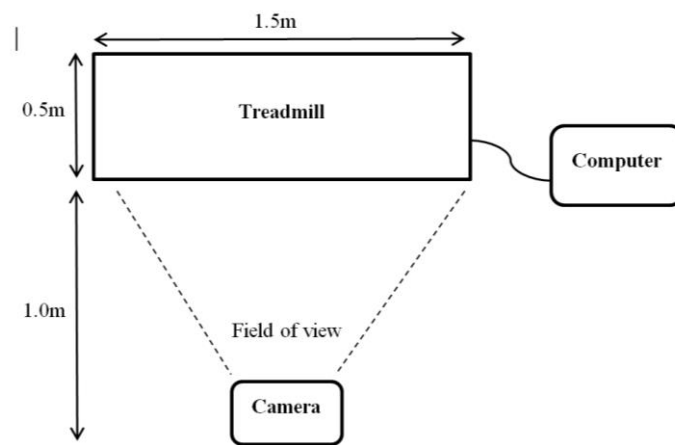


Figure 3.3: Top View of Setup for Data Acquisition.

3.3 Data Analysis

Data analysis was done using two different software. SkillSpector software was used as a motion capture system to acquire the trajectories of the markers and perform kinematic analysis to obtain linear and angular kinematic parameters such as joint angle, velocity, acceleration etc. The coordinates of the markers obtained from SkillSpector together with the force data obtained from Gaitway software were then used as input to perform kinetic analysis to obtain joint moment in the Microsoft Excel spread sheet.

3.3.1 Kinematic Analysis

In this analysis, the duration of analysis was defined as a complete gait cycle performed by the subject. Several gait cycles were captured during the 30 seconds of acquisition and only three gait cycle from each subject were selected for analysis. The video that contains walking movement was trimmed to contain only one gait cycle before being use in SkillSpector software for each time of analysis.

The SkillSpector software was downloaded from the Video4coach website. After opening the software, the first step is to define the human model and calibration object in the model wizard. In the window of defining a human model, the number of points to be digitized is the number of markers attached on the subject (Figure 3.4), while the assignments of point (Figure 3.5) and segment (Figure 3.6) names were done in the following windows. The magnitude of 2D calibration object was defined by numerous points (Figure 3.7) in the calibration wizard. After defining the model and calibration object, the next step is to digitize the model (Figure 3.8) and the calibration object (Figure 3.9) in video sequence. After digitizing was done, the image coordinates were transformed into real world coordinate with the DLT algorithm and kinematic parameters were calculated.

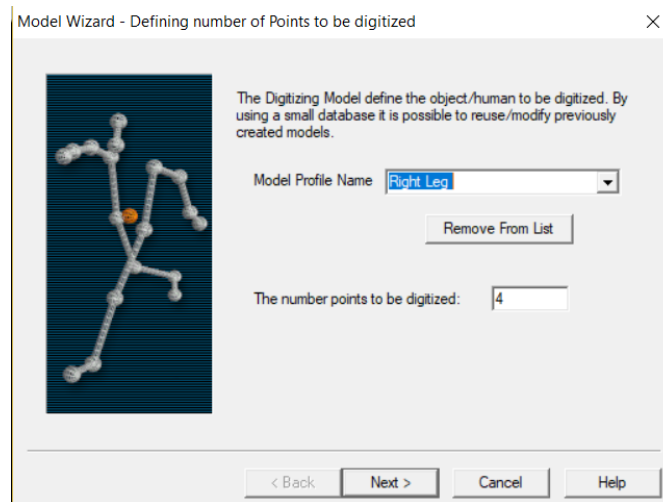


Figure 3.4: Defining Number of Points to be Digitized.

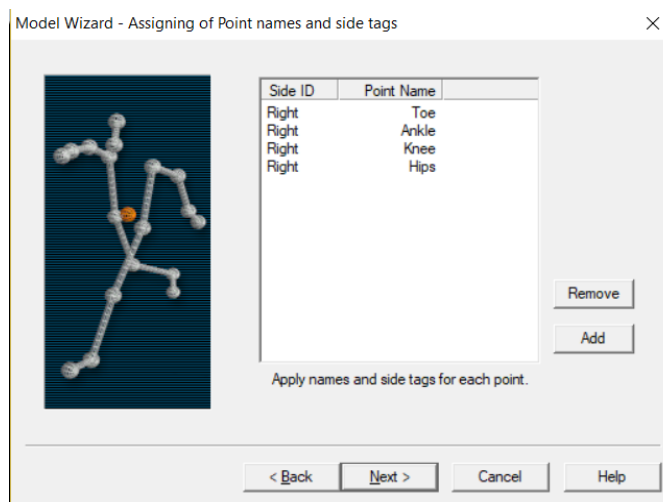


Figure 3.5: Assigning Point Names.

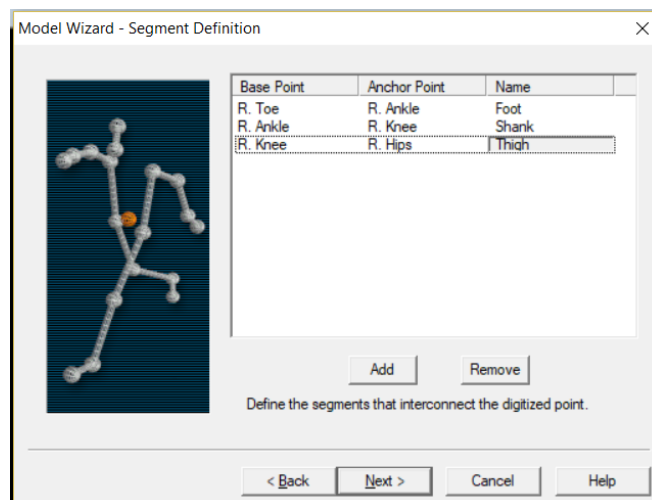


Figure 3.6: Defining Segments.

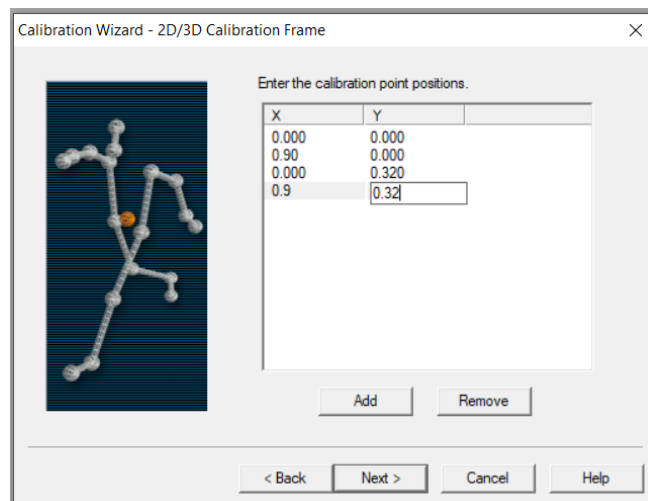


Figure 3.7: Defining Calibration Points.

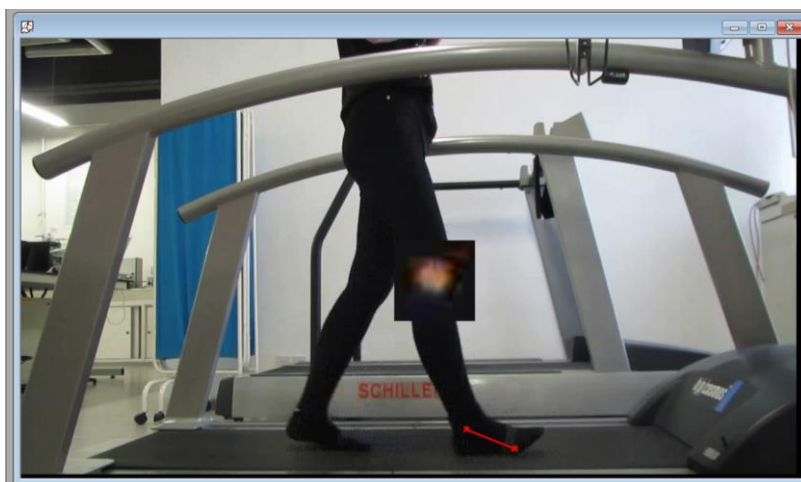


Figure 3.8: Digitizing Movement.



Figure 3.9: Digitizing Calibration.

The next step is to perform filtering on the raw kinematic data (Figure 3.10). Due to the presence of noise mainly caused by skin movement artefacts and improper digitization of markers (Winter et al., 1974), the kinematic data must be low pass filtered prior to performing further analysis. The conventional practice is that kinematic data are filtered at cut-off frequency of 6 Hz (Krupenevich, n.d.). Therefore, in this work the raw kinematic data was filtered at cut-off frequency of 6 Hz.

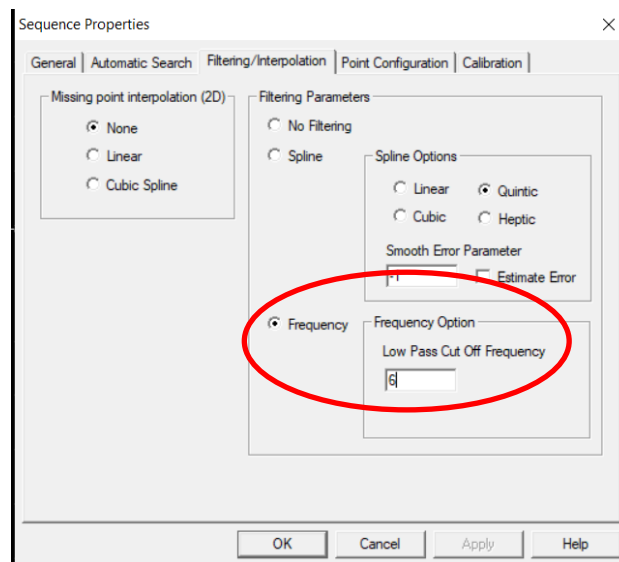


Figure 3.10: Setting Filtering Parameters.

The output of the SkillSpector combines the video, animation and kinematic information in one window, as illustrated in Figure 3.11. The progression of animation and kinematic information were observed by navigating the video. The linear and angular data produced in the kinematic analysis were then export as text file for further analysis.

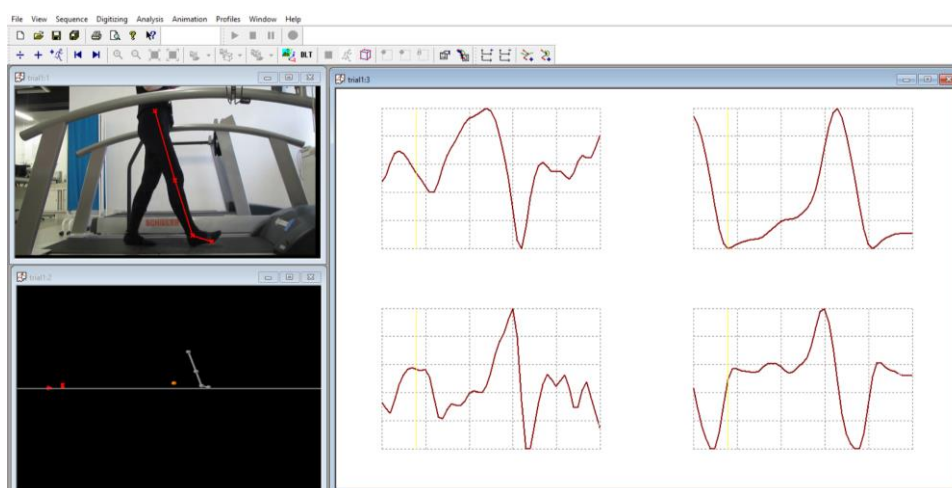


Figure 3.11: Output of SkillSpector.

3.3.2 Kinetic Analysis

After obtaining the linear and angular kinematics data from SkillSpector, the outputs were used as inputs to calculate joint moments by Classical Newton-Euler methodology of inverse dynamics in the Microsoft Excel spreadsheet.

The classical Newton-Euler equation (Equation 2.1 and Equation 2.2) calculates the moment of the joints starting from the most distal joint and move inwards along the kinematic chain of an open loop structure. The classical Newton-Euler methodology only applies for open-loop structures, for close loop structures, the equation become useless (Oliveira, 2016). Since walking movement is a closed-loop structure, the equation needs to be customised in order to include the ground reaction force produced during contact of the limb to ground. The basic concept of Newton-Euler methodology in calculating joint moment during walking is illustrated in Equation 3.1.

$$\text{joint moment} = \text{total moment} - \text{ground reaction moment} - \text{joint reaction moment} \quad (3.1)$$

Newton-Euler equation (Equation 3.2, Equation 3.3, Equation 3.4) together with the sagittal plane link-segment model combined with free body diagram (FBD) of the right leg (Figure 3.12) proposed by Kirtley (2006) was adopted in this work to calculate proximal joint moment. The FBD consists of

three segments (foot, shank and thigh) linked together by the joints where the markers were located at the MTP5, ankle, knee and hip.

$$R_{xp} = m_z a_x - R_{xd} \quad (3.2)$$

$$R_{yp} = m_z a_y + m_z g - R_{yd} \quad (3.3)$$

$$M_{zp} = I_z \alpha_z - M_{zd} - R_{xp}(Y_p - Y_{CoM}) + R_{yp}(X_{CoM} - X_p) + R_{xd}(Y_{CoM} - Y_d) - R_{yd}(X_d - X_{CoM}) \quad (3.4)$$

where

m_z = segment mass, kg

R = reaction force, N

x = x-direction

y = y-direction

p = proximal

d = distal

*Note that when p = ankle joint, d = force platform

a = acceleration of CoM, m/s²

$g = 9.81\text{m/s}^2$

M_z = joint moment, N·m

I_z = segment mass moment of inertia, kg·m²

α_z = segment angular acceleration, rad/s²

CoM = Centre of Mass

CoP = Centre of Pressure

X = x-coordinate

Y = y-coordinate

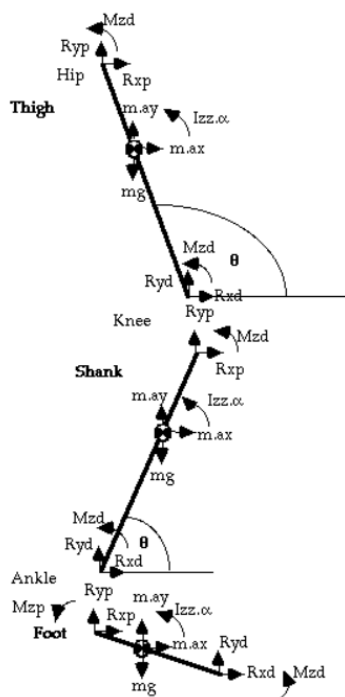


Figure 3.12: 2D Sagittal Plane FBD (Kirtley, 2006).

For anthropometric parameters estimation such as segment mass, length, distance of segment CoM to proximal or distal joint used in inverse dynamics calculation of lower extremity, the information in Table 3.1 formed by Dempster (1955) and Dempster, Gabel and Felts (1959) was used. Although estimation methods are more error-prone than functional methods, they provide an easier way of implementation and eliminate the needs of recording additional motions (Oliveira, 2016). In addition, some of these anthropometric parameters are not possible to be measured directly.

Table 3.1: Anthropometric Parameter Estimation.

Segment	Segment Mass (m_{ratio})	Location of CoM (L_{ratio})		Radius of Gyration/ Segment Length (ρ_{ratio})		
		proximal	distal	CoM	Proximal	Distal
Foot	0.0145M	0.50	0.50P	0.475	0.69	0.690P
Shank	0.0465M	0.433	0.567P	0.302	0.528	0.643M

In order to perform inverse dynamics, few parameters such as mass of segments, location of CoM, gyration radius need to be calculated before the Newton-Euler equation can be applied. The equations are expressed by Equation 3.5 to Equation 3.10.

First of all, the segment mass was calculated as Equation 3.5 as a percentage of total body mass.

$$m_z = m_{ratio} \times m_{total} \quad (3.5)$$

where

m_{ratio} = ratio of segment mass to total body mass

m_{total} = total body mass

From the output of SkillSpector, the marker coordinates represented in X and Y values were used to calculate the coordinate of CoM of each segment using Equation 3.6 and Equation 3.7.

$$X_{CoM} = X_p + L_{ratio.p} \times (X_d - X_p) \quad (3.6)$$

$$Y_{CoM} = Y_p - L_{ratio.p} \times (Y_p - X_d) \quad (3.7)$$

where

$L_{ratio.p}$ = ratio of distance of CoM from proximal joint

Equation 3.8, Equation 3.9 and Equation 3.10 show the calculation of the radius of gyration at the segment CoM.

$$L_z = \sqrt{(X_p - X_d)^2 + (Y_p - Y_d)^2} \quad (3.8)$$

$$\rho_z = L_z \times \rho_{ratio.CoM} \quad (3.9)$$

where

L_z = length of segment

ρ_z = radius of gyration from CoM to proximal joint

$\rho_{ratio.CoM}$ = ratio of gyration radius to total segment length

The moments of inertia of segments according to their respective CoM were calculated in Equation 3.10.

$$I_z = m_z \times \rho_z^2 \quad (3.10)$$

After obtaining all the required parameters, the joint reaction forces and moments were solved following the kinematic chain, starting with the ankle to knee. From the Newton equation, the horizontal (Equation 3.11 and Equation 3.14) and vertical (Equation 3.12 and Equation 3.15) elements of the joint reaction force were calculated. From the Euler Equation, the joint moments were calculated using Equation 3.13 and Equation 3.16. As mentioned earlier, the treadmill that was used in this research only provides vertical ground reaction data without horizontal ground reaction data, hence Equation 3.11 and Equation 3.13 precludes the horizontal ground reaction force. In addition, the treadmill that was used also did not provide any information on the location of centre of pressure (CoP) which is required in Equation 3.13, hence assumptions on the location of CoP as shown in Table 3.2 was made while performing calculation of ankle joint moment.

Table 3.2: Assumptions Made on Location of CoP.

Gait term	Location of CoP
Heel Strike	Heel
Flat Foot	Location of foot CoM
Midstance	Location foot CoM
Heel Off	Ball of foot

Ankle:

$$R_{ankle.x} = m_{foot} a_{foot.x} \quad (3.11)$$

$$R_{ankle.y} = m_{foot} a_{foot.y} + m_{foot} g - R_{VGRF} \quad (3.12)$$

$$M_{ankle} = I_{foot} \alpha_{foot} - R_{ankle.x} (Y_{ankle} - Y_{foot.CoM}) + R_{ankle.y} (X_{foot.CoM} - X_{ankle}) - R_{VGRF} (X_{ankle} - X_{foot.CoP}) \quad (3.13)$$

Knee:

$$R_{knee.x} = m_{shank}a_{shank.x} - R_{ankle.x} \quad (3.14)$$

$$R_{knee.y} = m_{shank}a_{shank.y} + m_{shank}g - R_{ankle.y} \quad (3.15)$$

$$M_{knee} = I_{shank}\alpha_{shank} - M_{ankle} - R_{knee.x}(Y_{knee} - Y_{shank.CoM}) + R_{knee.y}(X_{shank.CoM} - X_{knee}) + R_{ankle.x}(Y_{shank.CoM} - Y_{ankle}) - R_{ankle.y}(X_{ankle} - X_{shank.CoM}) \quad (3.16)$$

3.3.3 Statistical Analysis

After obtaining all the outputs from kinematic and kinetic analysis, the mean and standard deviation of peak values of each parameter of each subject were calculated with Equation 3.17 and Equation 3.18.

$$\bar{x} = \frac{\Sigma x}{N} \quad (3.17)$$

$$\sigma = \sqrt{\frac{\Sigma(x-\bar{x})^2}{N}} \quad (3.18)$$

where

\bar{x} = mean

x = value of data

N = number of data

σ = standard deviation

CHAPTER 4

RESULTS AND DISCUSSIONS

4.1 Introduction

The results of gait analysis will be discussed in this chapter. Section 4.2 discussed about the kinematics and kinetic analysis on joint angles and moments. Section 4.3 further evaluated the reliability of the output by comparing the factors that affect the magnitude of the kinematic and kinetic parameters. In Section 4.4, the difference between CoM and CoP were discussed to avoid any confusion of the two terms in calculating joint moments.

4.2 Data Validation

This section of the report discussed about the output of analysis. The result from the kinematic and kinetic analysis will be evaluated by comparing with results established by other researchers.

4.2.1 Kinematic Parameters

The kinematic analysis of ankle and knee joint from SkillSpector software will be discussed in this section. The original output from SkillSpector software provides the joint angle in a relative manner. In order to compare with the results established by other researches, the relative angles were converted into absolute angles.

Figure 4.1 shows the how the measurement of ankle joint absolute angle was done. Figure 4.2 and Figure 4.3 are the graphs of ankle joint angle against percentage of gait plotted from analysis whereas Figure 4.4 presents graphs of ankle joint angle in sagittal plane published by other researchers.

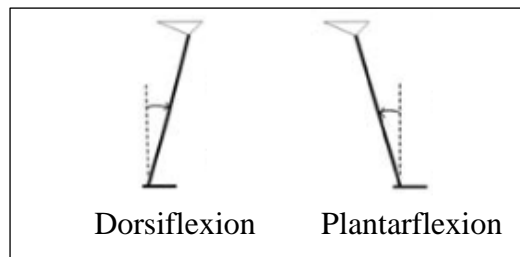


Figure 4.1: FBD for Measurement of Ankle Joint Angle (Perry and Davids, 1992).

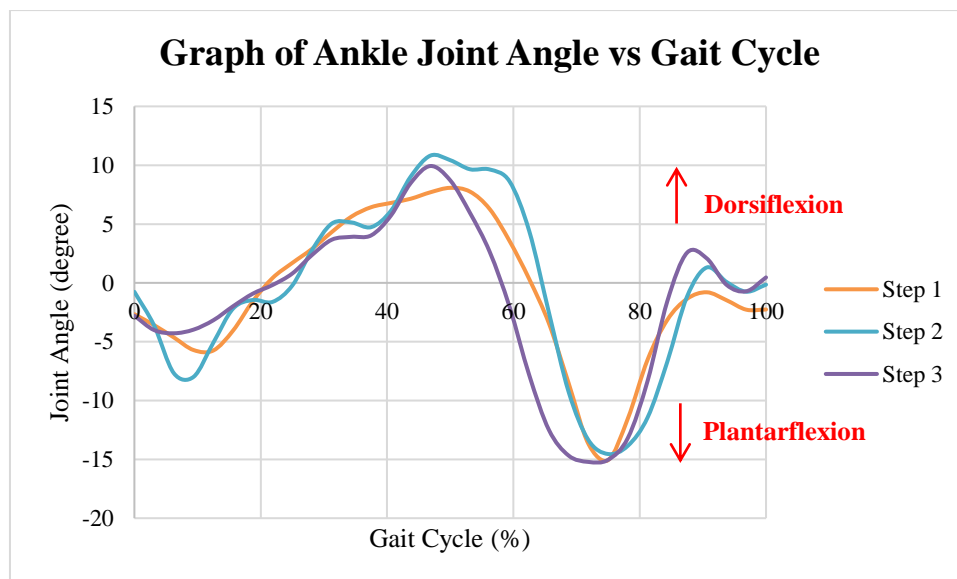


Figure 4.2: The Graph of Ankle Joint Angle against Percentage of Gait Plotted from Analysis for Female Subject.

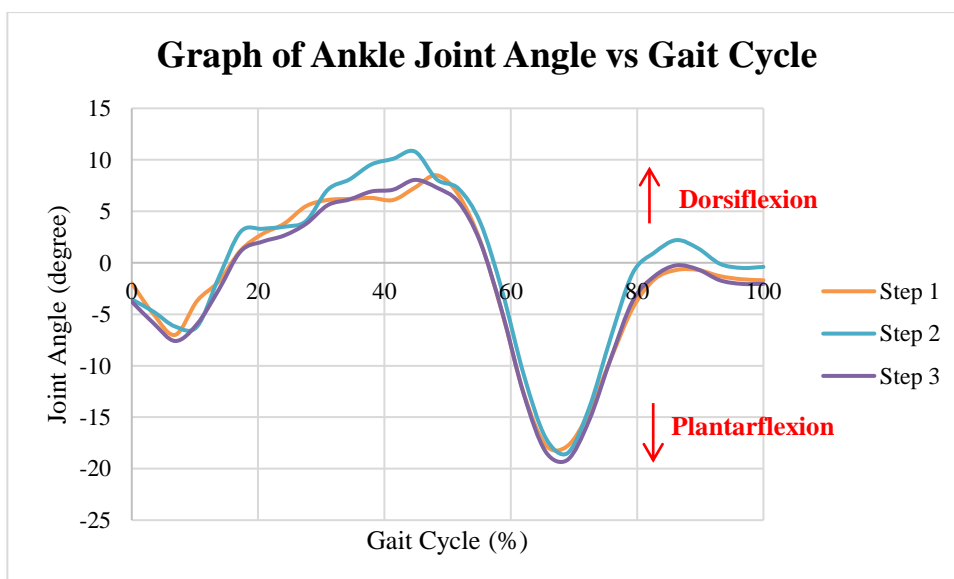


Figure 4.3: The Graph of Ankle Joint Angle against Percentage of Gait Plotted from Analysis for Male Subject.

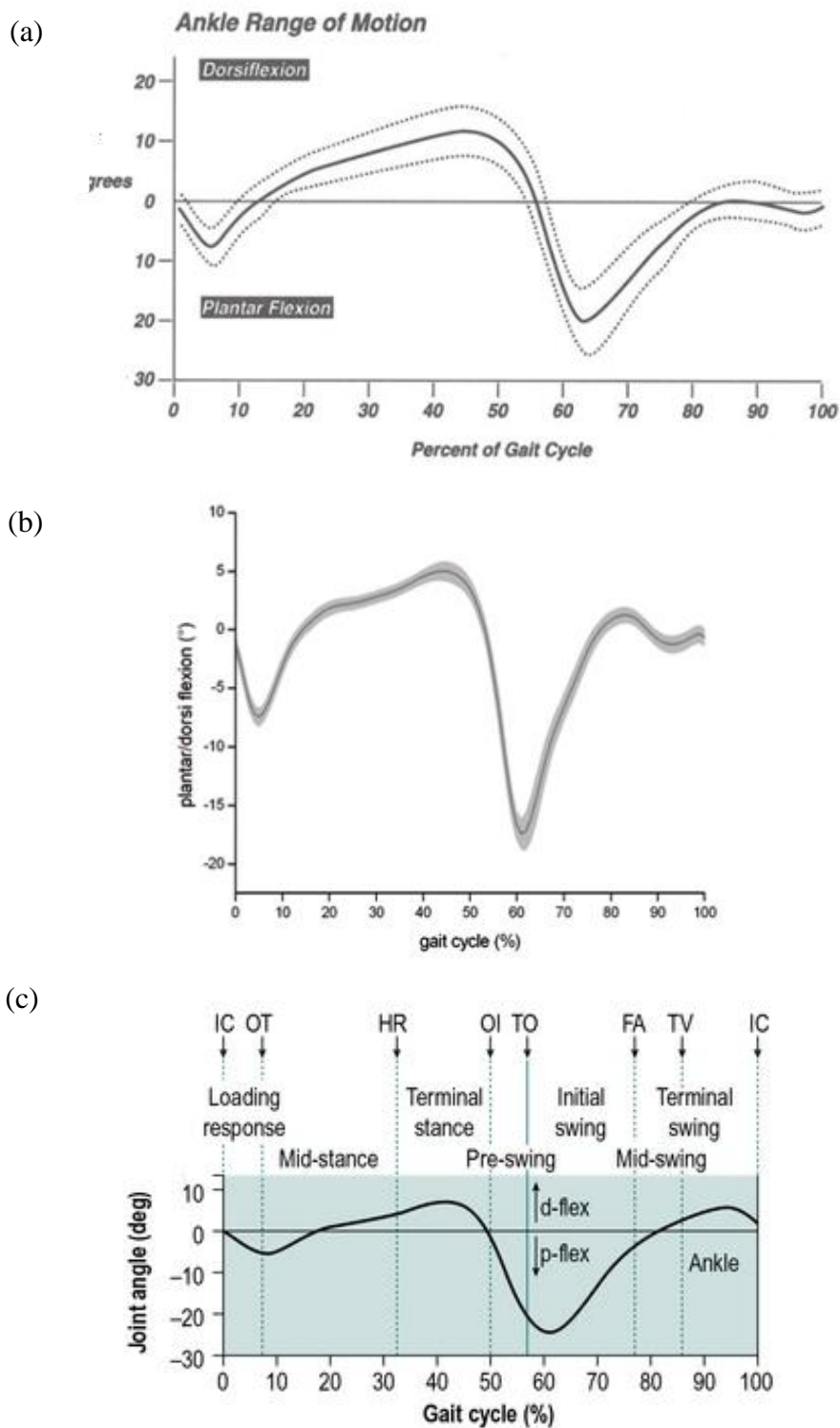


Figure 4.4: (a) Ankle Range of Motion for a Gait Cycle (Perry and Davids, 1992). (b) Ankle Joint Angle Measured using Electrogoniometer against Percentage of Gait in Sagittal Plane (Moriguchi, Sato and Gil Coury, 2007). (c) Sagittal Plane Ankle Joint Angle. IC = Initial Contact; HR = Heel Rise; TO = Toe Off (Musculoskeletal Key, 2016).

The curve pattern of the graphs in Figure 4.2 and 4.3 shows similar pattern with figure 4.4; initially the ankle experience plantarflexion and slowly convert into dorsiflexion until midstance to move body forward. Maximum dorsiflexion is achieved at the middle of push off period. Although the magnitude of angles might be different due to age of the subjects, gender of the subjects and gait speed (Oberg, Karsznia and Oberg, 1994), it is more important to focus on changes of variables, rather than the absolute values (Musculoskeletal Key, 2016).

Table 4.1 below shows the mean and standard deviation of the peak values of ankle joint angle for both female and male subject.

Table 4.1: Peak Values of Ankle Joint Angle.

Variable	Mean \pm Standard Deviation	
	Female	Male
Peak Dorsiflexion	9.61 \pm 1.40	9.12 \pm 1.48
Peak Plantarflexion	14.94 \pm 0.35	18.48 \pm 0.68

According to publication by Stauffer, Chao and Brester (1977), normal healthy subjects have overall walking range of motion in the sagittal plane between 20 and 31 degree, moving from 6 to 16 degree for dorsiflexion and 13 to 17 degree for plantarflexion. This research had recruited five young (mean age 29), healthy (no history of complaints related to ankle joint) male volunteers to walk on a 9-meter walkway in their regular shoes at own preferable speed. The results obtained from the analysis are within the range published by this research paper. Although the magnitude of plantarflexion of the male subject is slightly greater than the range published, it is believed that it was caused by the difference between barefoot condition and shoe condition.

Figure 4.5 shows the how the measurement of knee joint absolute angle was done. Figure 4.6 and Figure 4.7 are the graphs of knee joint angle against percentage of gait plotted from analysis whereas Figure 4.8 presents graphs of knee joint angle in sagittal plane published by other researchers.

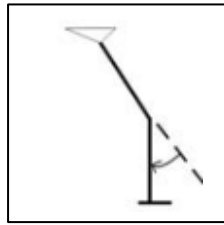


Figure 4.5: FBD for Measurement of Knee Joint Absolute Angle (Perry and Davids, 1992).

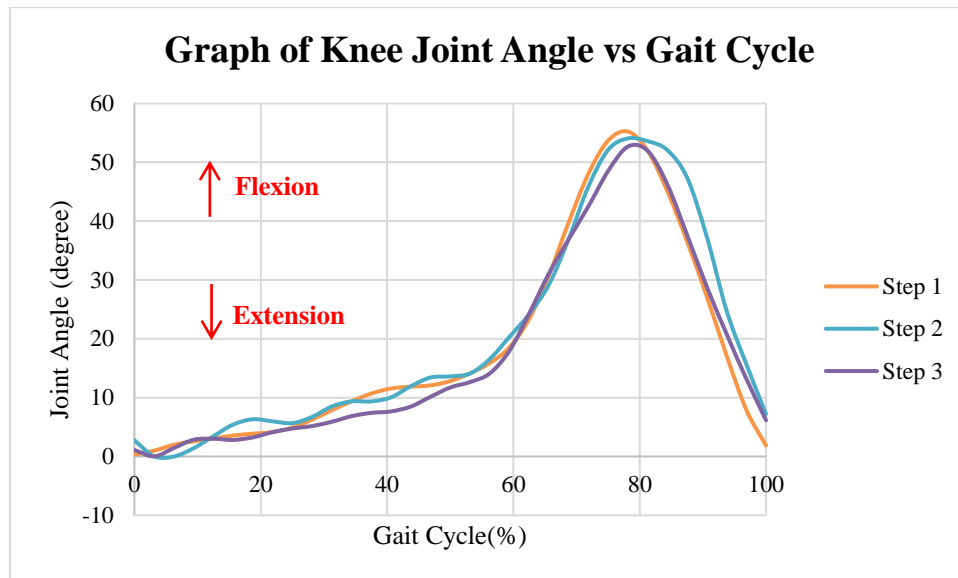


Figure 4.6: The Graph of Knee Joint Angle against Percentage of Gait Plotted from Analysis for Female Subject.

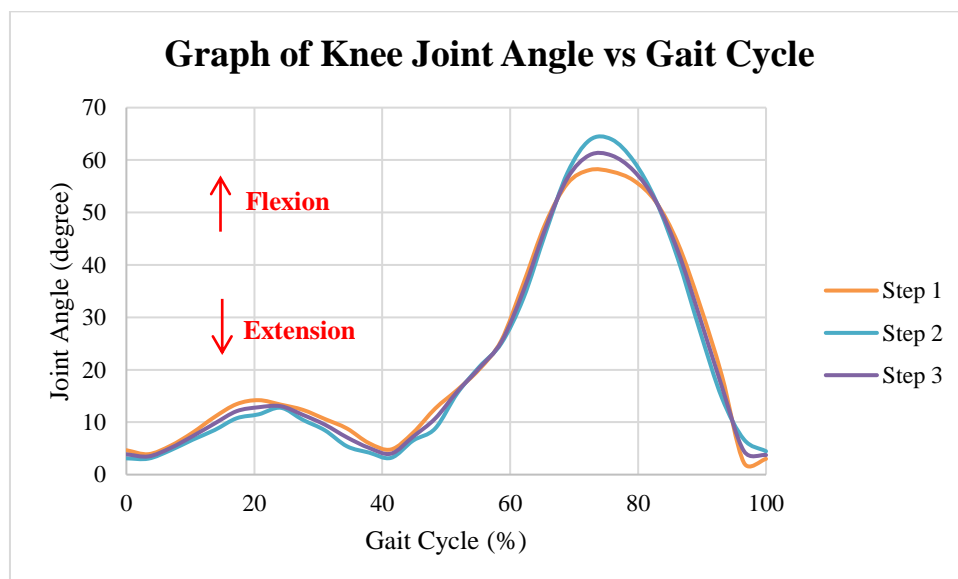


Figure 4.7: The Graph of Knee Joint Angle against Percentage of Gait Plotted from Analysis for Male Subject.

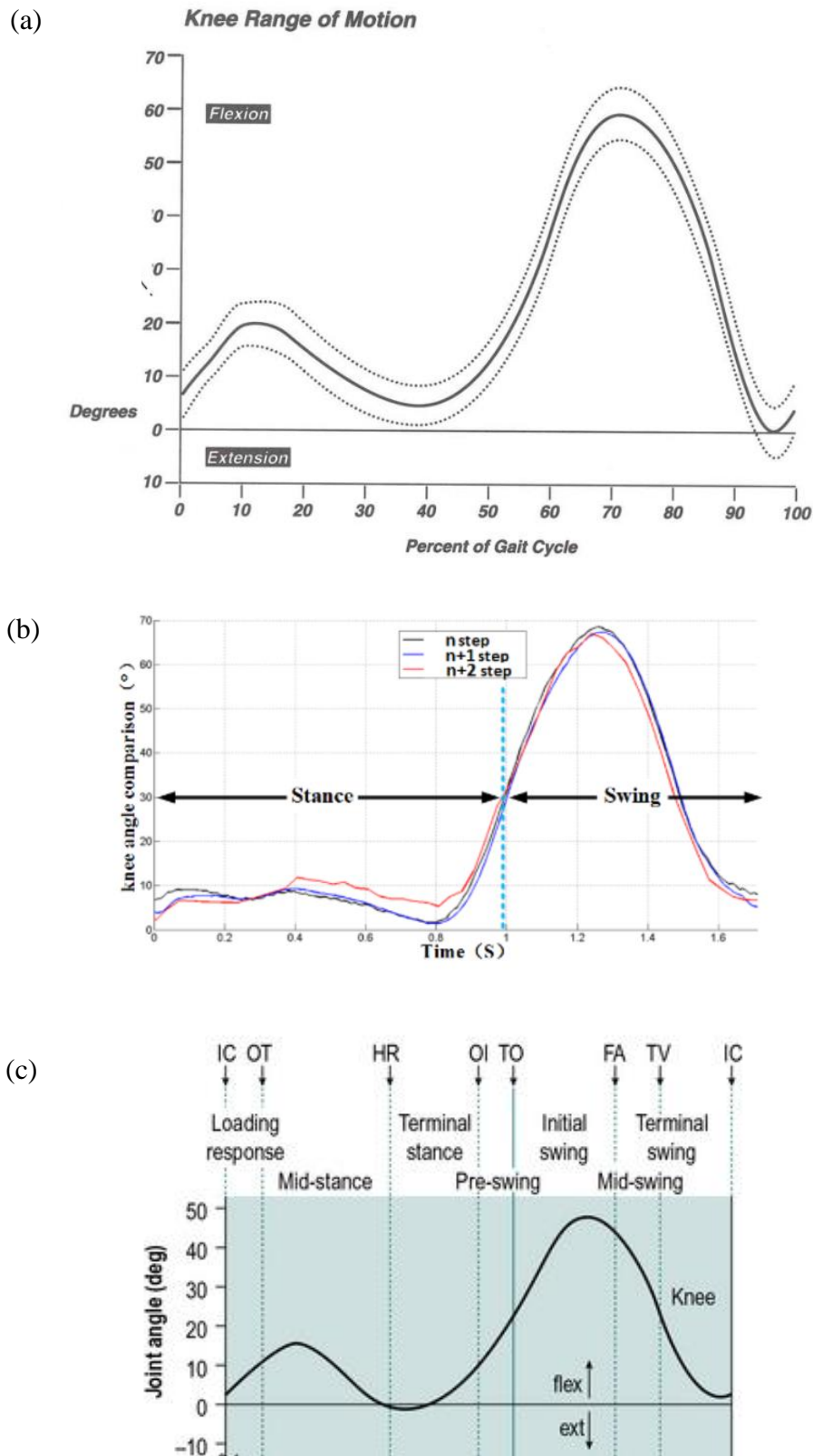


Figure 4.8: (a) Knee Range of Motion for a Gait Cycle (Perry and Davids, 1992). (b) Changes in Angle of Knee Flexion during Linear Walking (Qiu, et al., 2017). (c) Sagittal Plane Knee Joint Angle (Musculoskeletal Key, 2016).

The curve pattern in Figure 4.8 describes the knee joint angle during where initially the knee joint experience flexion and maximum extension during at the heel rise. Maximum flexion is achieved during swing phase and maximum knee extension at second heel strike. All graphs in Figure 4.6, Figure 4.7 and Figure 4.8 shows maximum knee flexion during swing phase and maximum knee extension at the second contact of foot with ground. However, in Figure 4.6, the graph plotted from analysis of female subject does not show any significant decrease in knee joint angle at heel rise. After checking the video, it was observed that the straightening of shank of subject prior to heel rise was not significant, hence the trough occurs during heel rise at knee joint angle was absent.

Table 4.2 below shows the mean and standard deviation of the peak values of knee joint angle for both female and male subject.

Table 4.2: Peak Values of Knee Joint Angle.

Variable	Mean \pm Standard Deviation	
	Female	Male
Maximum Flexion	53.98 \pm 1.28	61.00 \pm 2.93

According to a publication by Oberg, Karsznia and Oberg (1994), a normal healthy male has a knee joint angle within the range of 56.7 to 77.1 degree while a normal healthy female has a knee joint angle within the range of 51.1 to 74.9 degree during swing phase of walking gait. This research had recruited 233 subjects (116 male and 117 women), aged 10-79 and subjects were instructed to walk on a 10-meter walkway with their own preferable speed. The results obtained from the analysis fall within the range published by this research paper.

4.2.2 Kinetic Parameters

The kinetic analysis of ankle and knee joint from inverse dynamics model done in the Microsoft Excel spread sheet will be discussed in this section.

Figure 4.9 shows the convention for ankle joint moment. Figure 4.10 and Figure 4.11 shows the graphs of ankle joint moment against percentage of gait

plotted from analysis whereas Figure 4.12 presents graphs of ankle joint moment in sagittal plane published by other researchers.

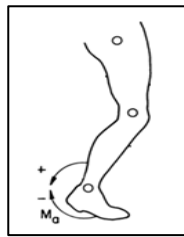


Figure 4.9: Convention for Ankle Joint Moment.

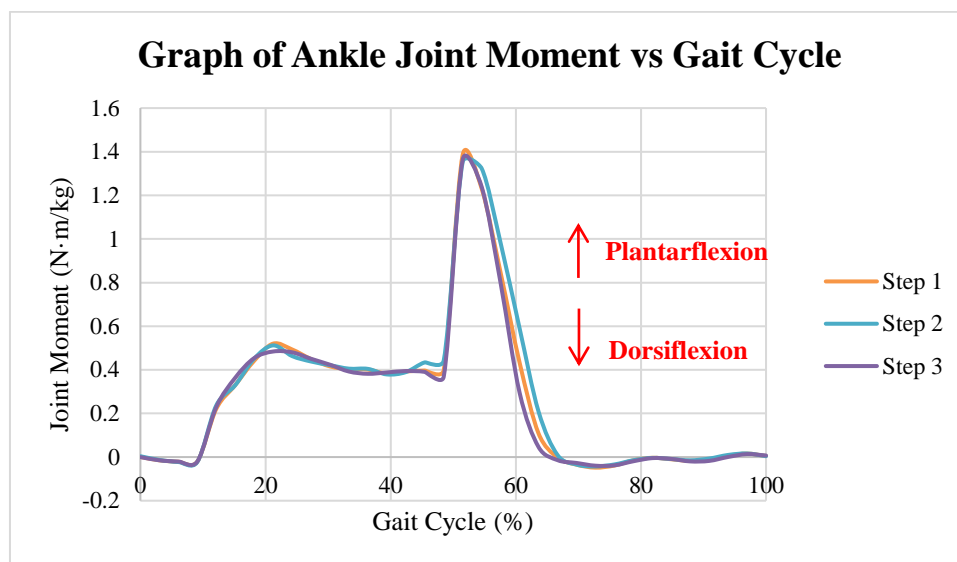


Figure 4.10: The Graph of Ankle Joint Moment against Percentage of Gait Plotted from Analysis for Female Subject.

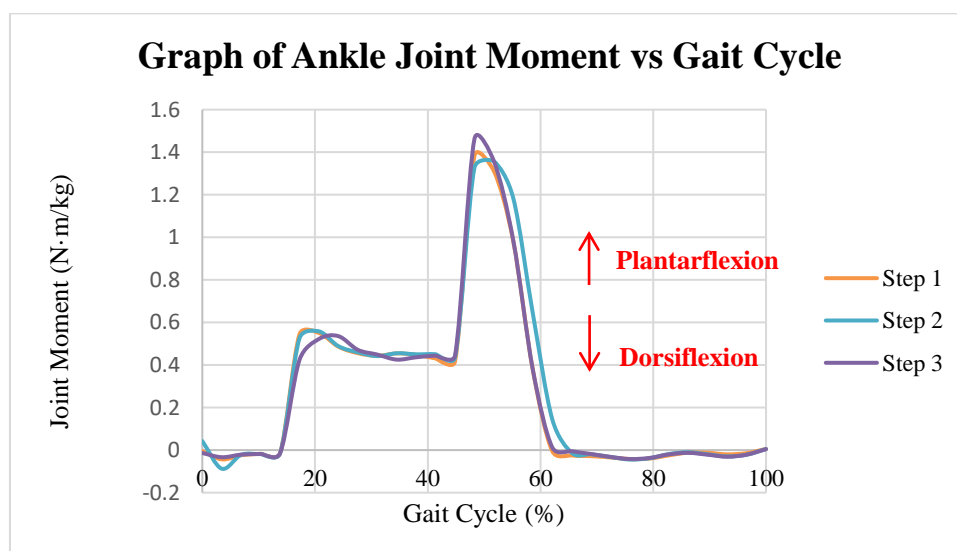
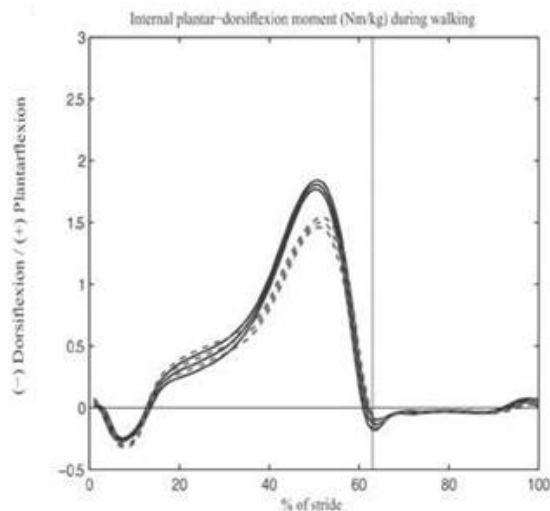
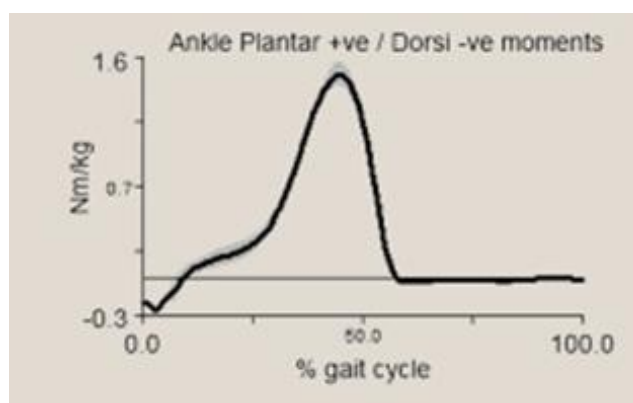


Figure 4.11: The Graph of Ankle Joint Moment against Percentage of Gait Plotted from Analysis for Male Subject.

(a)



(b)



(c)

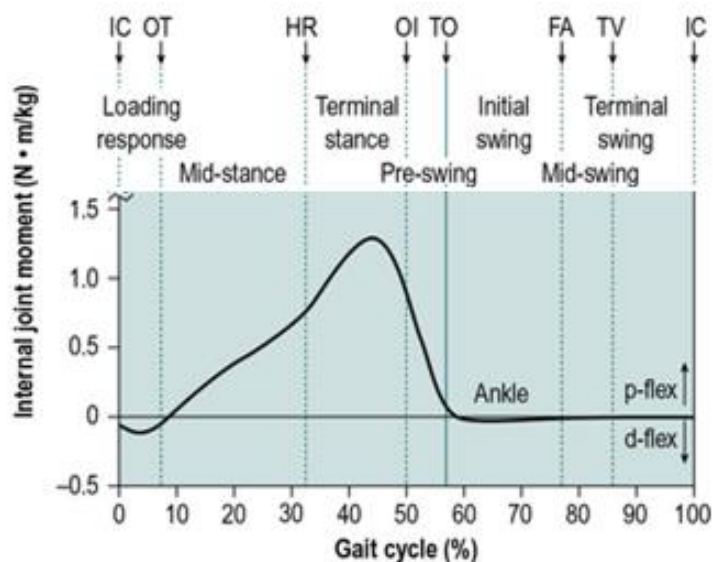


Figure 4.12: (a) Sagittal Plane Internal Joint Moments of Ankle during Walking (Sobhani, Dekker, Postema and Dijkstra, 2012). (b) Sagittal Plane Ankle Moments from Gait Analysis of Five Walking Trials (Brockett and Chapman, 2016). (c) Sagittal Plane Ankle Joint mMoment (Musculoskeletal Key, 2016).

The curve pattern of the graphs in Figure 4.10 and 4.11 shows similar pattern with Figure 4.12 except that the curves in Figure 4.10 and Figure 4.11 are less smooth compared to curves in Figure 4.11. This is due to the assumptions made for location of CoP which was discussed in the Section 3.3.2. From the curve patterns, it was observed that after initial contact, there is a small ankle dorsiflexion moment due to eccentric contraction of ankle dorsiflexors to pull the foot towards the shank to avoid foot from slapping onto the ground. A negative value was used to represent this anticlockwise rotation dorsiflexion moment. Then followed by ankle plantarflexion moment as the shank move towards the foot. During toe-off, large ankle plantarflexion moment was observed. The large ankle plantarflexion moment was due to concentric contraction of the ankle plantarflexors to push the body upwards.

Table 4.3 below shows the mean and standard deviation of the peak values of ankle joint moment for both female and male subject.

Table 4.3: Peak Values of Ankle Joint Moment.

Variable	Mean \pm Standard Deviation	
	Female	Male
Peak Plantarflexion	1.36 \pm 0.02	1.40 \pm 0.05

According to a study by Schache and Baker (2007), the mean peak stance plantarflexion moment for two adult men and seven adult women walking in their own preferable speed is 1.333 N·m/kg with a standard deviation of 0.122. The results obtained from the analysis was quite close to the range published by this research paper. In addition, according to Toda, Nagano and Luo (2015), young males have greater ankle dorsiflexion and plantarflexion moment than young females, hence the results from the analysis are acceptable.

Figure 4.13 shows the convention for knee joint moment. Figure 4.14 and Figure 4.15 are the graphs of knee joint moment against percentage of gait plotted from analysis whereas Figure 4.16 presents graphs of knee joint moment in sagittal plane published by other researchers.

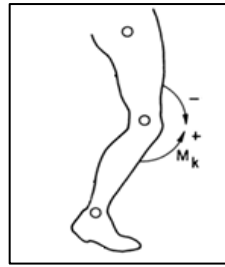


Figure 4.13: Convention for Knee Joint Moment.

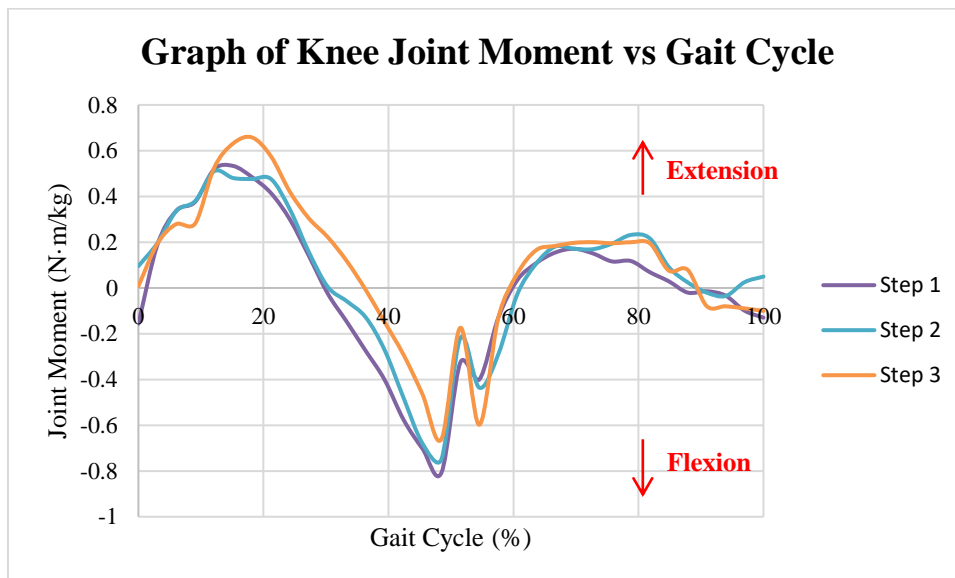


Figure 4.14: The Graph of Knee Joint Moment against Percentage of Gait Plotted from Analysis for Female Subject.

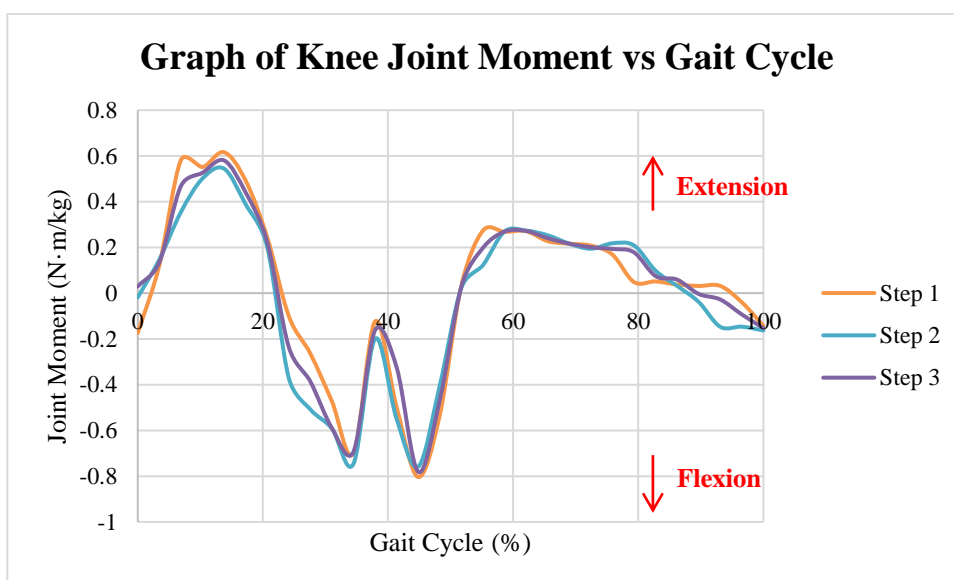


Figure 4.15: The Graph of Knee Joint Moment against Percentage of Gait Plotted from Analysis for Male Subject.

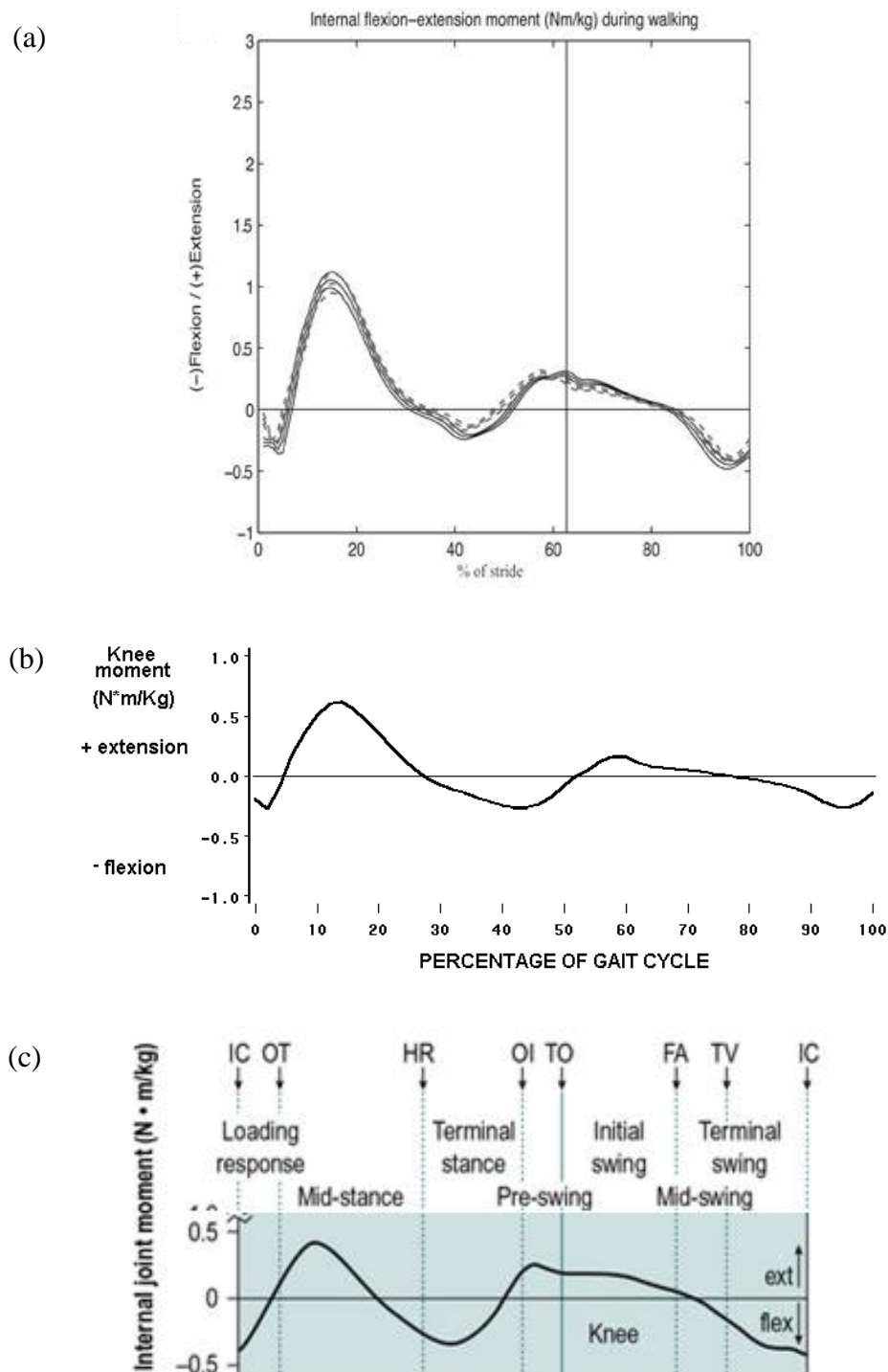


Figure 4.16: (a) Sagittal Plane Internal Joint Moments of Knee during Walking (Sobhani, Dekker, Postema and Dijkstra, 2012). (b) Moment at the Knee during the Gait Cycle (Winter, 1987). (c) Sagittal Plane Knee Joint Moment (Musculoskeletal Key, 2016).

Figure 4.14, Figure 4.15 and Figure 4.16 shows similar curve pattern except that curves in Figure 4.10 and Figure 4.11 are less smooth. From the curve patterns, it was observed that there are two peaks of knee flexion moment and two peaks knee extension moment for each gait cycle. After initial contact, there is a small knee flexion moment which is caused by eccentric contraction of the quadriceps due to vertical ground reaction. Then followed by a knee extension moment to allow progression of trunk towards the leg. During push-off, quadricep contract eccentrically to support the knee against the contraction of triceps resulting in a peak knee flexion moment and extends again before the next gait cycle start.

Table 4.2 below shows the mean and standard deviation of the peak values of knee joint moment for both female and male subject.

Table 4.4: Peak Values of Knee Joint Moment.

Variable	Mean \pm Standard Deviation	
	Female	Male
First Maximum Extension	0.56 \pm 0.08	0.58 \pm 0.04
Maximum Flexion	0.73 \pm 0.07	0.78 \pm 0.02
Second Maximum Extension	0.20 \pm 0.03	0.27 \pm 0.001

According to research by Schache and Baker (2007), the mean value for first maximum extension moment is 0.500 N·m/kg with a standard deviation of 0.220, maximum flexion moment is 0.215 N·m/kg with a standard deviation of 0.149 and second maximum extension moment is 0.269 N·m/kg with a standard deviation of 0.115. This experiment was carried out with two adult men and seven adult women walking in their own preferable speed. The results obtained from the analysis was within the range published by this research paper except that the analysis result shows a lower value of flexion moment at initial contact and larger value of flexion moment after heel rise.

The fact that the graph plotted from kinematic data obtained from analysis of SkillSpector software and graph plotted from kinetic data obtained from analysis of inverse dynamic model are able to reproduce similar curve pattern of graph established by other researchers have proven the reliability of

Skillspector software and inverse dynamic model in performing kinematic and kinetic analysis. However, assumptions made for location of CoP used in inverse dynamics calculation need to be further improvised to obtain a better result.

4.3 Factors Affecting Magnitude of Kinematic and Kinetic Data

This section of the report discusses about the factors affecting magnitude of the kinematic and kinetic parameters from the analysis. Age, gender, gait speed and type of footwear are the four most significant factor affecting the magnitude.

Various studies have showed significant differences in kinematic and kinetic variables as a function of age and type of footwear (Nigg, Fisher and Ronsky, 1994; Toda, Nagano and Luo, 2015). However, since the two subjects recruited for the experiment are about the same age and the experiment was carried out in barefoot condition, the factor of age and footwear will not be further reviewed.

According to Nigg, Fisher and Ronsky (1994) research, they had verified that young females (age of 20-39 years old) have higher ankle range of motion during compared to young males and according to Oberg, Karsznia and Oberg (1994) research, male had larger excursions than women during normal gait. However, the joint angle does not only depend on the gender of the subject, it is also dependent of gait speed. Oberg, Karsznia and Oberg (1994) further justified in their research that joint angle and gait speed have directly proportional relationship. In other words, increase in gait speed results in increased joint angles in all joints and gait phases.

According to a research by Toda, Nagano and Luo (2015), young males have greater ankle dorsiflexion and plantarflexion moment and lower knee flexion and extension moment compared to young females. On the other hand, a study by Brockett and Chapman (2016) stated that with increasing gait speed, the kinetic patterns will remain similar but with higher magnitudes.

The results of this paper are reliable when compare with the results of published paper. With a greater speed (3.2 km/h) the male subject shows a

larger excursion and greater joint moment in both ankle and knee joint compared to the female subject with lower speed (2.5 km/h).

4.4 Difference between CoM and CoP

The term center of pressure (CoP) is often misrepresented as center of mass (CoM). CoM of a body is the net point which the body's mass is distributed evenly in all directions, while CoP is totally independent of CoM. CoP is the net point of the VGRF from a force platform acting on the subject. This force is dependent on foot placement and neuromuscular control of the ankle joint muscles. Figure 4.17 shows a record of the CoM and CoP of body swaying back and forth while standing by Winter (2009). It was observed that CoP must continuously moving back and forth to regulate the CoM of the body; thus, the range of CoP must be greater than CoM.

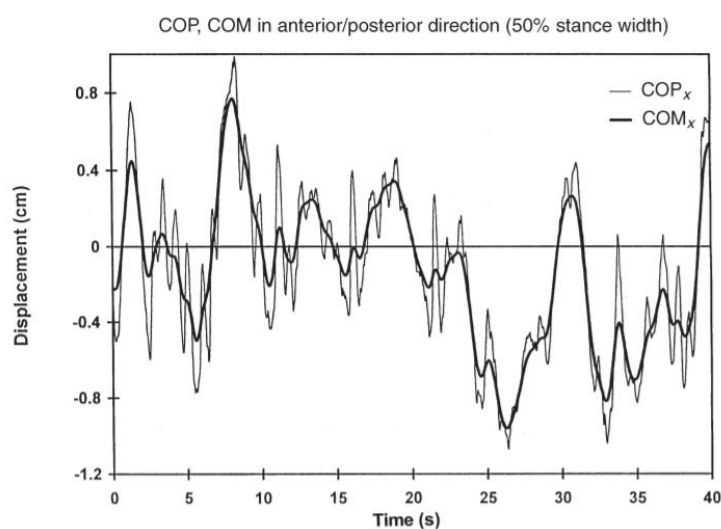


Figure 4.17: Record of CoM and CoP in Anterior Posterior Direction during Erect Standing (Winter, 2009).

Therefore, it can be deduced that misinterpretation of CoM and CoP can lead to inaccuracy in biomechanical analysis. The graph below (Figure 4.18) shows the comparison graph of ankle joint moment against percentage of gait plotted from analysis for female subject when CoM is misinterpreted as CoP. The blue line shows the graph plotted when the ankle joint moment was

calculated using CoP while the red line shows the graph plotted when the ankle joint moment was calculated using CoM.

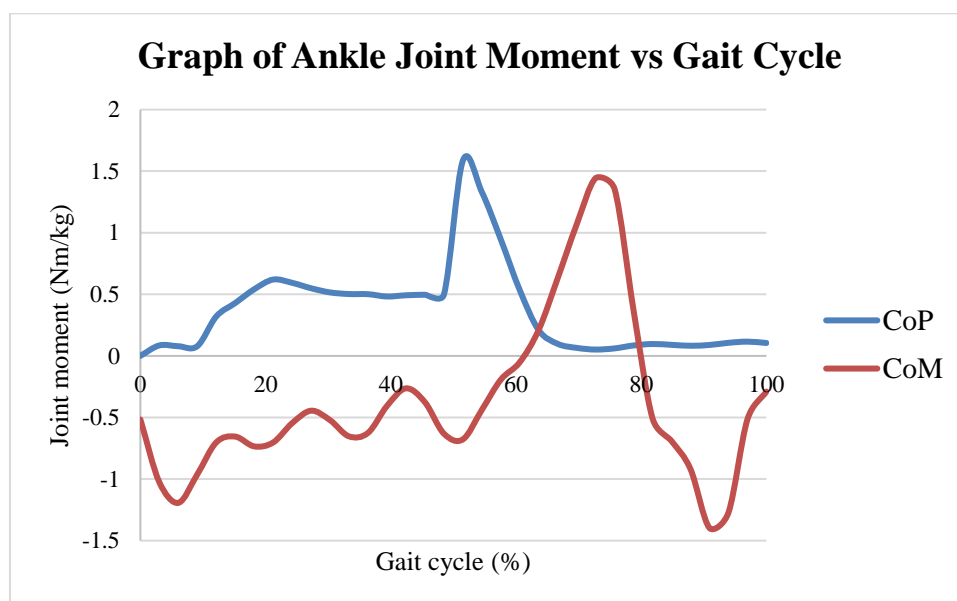


Figure 4.18: The Graph of Ankle Joint Moment against Percentage of Gait Plotted from Analysis for Female Subject when CoM is Misinterpreted as CoP (Red Line).

In typical cases, the CoP is measured using force plate when one foot or both feet are in contact with the ground. However, as mentioned, the treadmill used in this work was not able to give any information about the location of CoP, hence assumptions on the location of CoP was made (refer to Table 3.2) which caused the graph plotted from the analysis to be less smooth.

4.5 Summary

In this part of the report, the performance of the SkillSpector software and inverse dynamics model was evaluated against the previous literature findings. It has been observed that the kinetic and kinematic graph plotted from the analysis shows similar curve pattern with the results established by other researchers. One of the main reasons that contribute to error is the assumptions made due to limitations of the treadmill used.

In short, SkillSpector software and inverse dynamic model can cooperate with each other to provide reliable kinematic and kinetic analysis.

CHAPTER 5

CONCLUSIONS AND RECOMMENDATIONS

5.1 Conclusions

In a nutshell, the system proposed in this paper comprise a digital camera, a split-belt instrumented treadmill (H/P Cosmos™ Instrumented Treadmill) and a personal computer equipped with Gaitway software and SkillSpector Software. Inverse dynamic model was incorporated to perform the kinetic analysis. Despite of limitations of this project, an alternative for human gait modelling and analysis using low cost resources was developed. Yet, the proposed model is able to reproduce reliable outputs that are comparable to the existing results.

5.2 Recommendation for future work

To obtain a high accuracy analysis output, a 3D analysis on the whole human body is essential because a 2D analysis can cause loss of movement characteristics in other planes. In current study, the gait analysis had only been carried out in the sagittal plane. In future, kinematics and kinetics analysis at the other planes such as frontal and transverse plane should be incorporated. The SkillSpector software is capable to perform 3D motion analysis by using more than one camera to capture the gait movement. However, efforts must be made to synchronise the cameras to make sure all cameras are capturing videos in the same instance of time to avoid any errors.

Additionally, force plate that is capable to acquire ground reaction force in all horizontal and vertical direction is highly recommended. This is because ground reaction forces information serves as important input of inverse dynamics model in calculating joints moment. In addition, horizontal ground reaction force is also important to determine the location of CoP.

Lastly, in order to reduce the errors caused by mistake in determining joint position, active and passive markers are recommended to replace the sticker marker. Active and passive markers are very suitable to be used for

human kinematics measurements as they are easier to be detected in the motion capture system.

REFERENCES

- Abad, J.D., 2018. Ergonomics and simulation-based approach in improving facility layout. *Journal of Industrial Engineering International*, pp.1-9.
- Abass, S.J. and Faihan, B.A., 2015. Dynamic Analysis of the Gait Cycle for Normal and Abnormal Subjects. *Al-Nahrain Journal for Engineering Sciences*, 18(2), pp.343-350.
- Ahn, J. and Hogan, N., 2012. Walking is not like reaching: evidence from periodic mechanical perturbations. *PloS one*, 7(3), p.e31767.
- Alkjaer, T., Simonsen, E.B. and Dyhre-Poulsen, P., 2001. Comparison of inverse dynamics calculated by two-and three-dimensional models during walking. *Gait & Posture*, 13(2), pp.73-77.
- Bachynskyi, M., Oulasvirta, A., Palmas, G. and Weinkauff, T., 2014, April. Is motion capture-based biomechanical simulation valid for HCI studies?: study and implications. *Proceedings of the SIGCHI Conference on Human Factors in Computing Systems*, pp.3215-3224. AGM.
- Bajelan, S. and Azghani, M.R., 2014. Musculoskeletal modeling and simulation of three various Sit-to-Stand strategies: An evaluation of the biomechanical effects of the chair-rise strategy modification. *Technology and Health Care*, 22(4), pp.627-644.
- Brockett, C.L. and Chapman, G.J., 2016. Biomechanics of the ankle. *Orthopaedics and trauma*, 30(3), pp.232-238.
- Camomilla, V., Cereatti, A., Cutti, A.G., Fantozzi, S., Stagni, R. and Vannozzi, G., 2017. Methodological factors affecting joint moments estimation in clinical gait analysis: a systematic review. *Biomedical engineering online*, 16(1), p.106.
- Castelli, A., Paolini, G., Cereatti, A. and Della Croce, U., 2015. A 2D markerless gait analysis methodology: validation on healthy subjects. *Computational and mathematical methods in medicine*, 2015.

Chauhan, R.B. and Vyas, J.B., 2013. FES-Aid Walking For Paraplegic Patient By Using Musculoskeletal Modeling Software And Matlab. *International Journal Of Engineering Trends And Technology (IJETT)-Volume4Issue4-April*.

da Rocha, E.S., Machado, Á.S., Franco, P.S., Guadagnin, E.C. and Carpes, F.P., 2013. Gait asymmetry during dual-task obstacle crossing in the young and elderly. *Human Movement, 14*(2), pp.138-143.

das Virgens Chagas, D., Leporace, G., Praxedes, J., Carvalho, I., Pinto, S. and Batista, L.A., 2013. Analysis of kinematic parameters of gait in Brazilian children using a low-cost procedure. *Human Movement, 14*(4), pp.340-346.

Debaere, S., Delecluse, C., Aerenhouts, D., Hagman, F. and Jonkers, I., 2015. Control of propulsion and body lift during the first two stances of sprint running: a simulation study. *Journal of sports sciences, 33*(19), pp.2016-2024.

Delp, S.L., Anderson, F.C., Arnold, A.S., Loan, P., Habib, A., John, C.T., Guendelman, E. and Thelen, D.G., 2007. OpenSim: open-source software to create and analyze dynamic simulations of movement. *IEEE transactions on biomedical engineering, 54*(11), pp.1940-1950.

Dempster, W.T., 1955. *Space requirements of the seated operator, geometrical, kinematic, and mechanical aspects of the body with special reference to the limbs*. Michigan State Univ East Lansing.

Dempster, W.T., Gabel, W.C. and Felts, W.J., 1959. The anthropometry of the manual workspace for the seated subject. *American journal of physical anthropology, 17*(4), pp.289-317.

Fandaklı, S.A., Okumuş, H.İ. and Öztürk, M., 2018, October. A Study of Human Walking Biomechanics for Ankle-Foot Prosthesis Design. In *2018 6th International Conference on Control Engineering & Information Technology (CEIT)* (pp. 1-5). IEEE.

Hamandi, S.J., Azzawi, M. and Abdulwahed, W., 2018. Gait Analysis after Unilateral Total Hip Replacement Surgery. *Al-Nahrain Journal for Engineering Sciences*, 21(4), pp.458-466.

Hickox, L., 2014. Exploration of the Validity of the Two-Dimensional Sagittal Plane Standing Long Jump Model.

Hinrichs, R.N., 1985. Regression equations to predict segmental moments of inertia from anthropometric measurements: an extension of the data of Chandler et al.(1975). *Journal of Biomechanics*, 18(8), pp.621-624.

Hirunrat, S. and Ingkatecha, O., 2015. Kinematics and Kinetics of Jumping Serve in Youth National and National Thai Female Volleyball Players of Thailand.

Hisham, N.A.H., Nazri, A.F.A., Madete, J., Herawati, L. and Mahmud, J., 2017. Measuring ankle angle and analysis of walking gait using Kinovea. In *International Medical Device and Technology Conference* (pp. 247-250).

Holzbaur, K.R., Murray, W.M. and Delp, S.L., 2005. A model of the upper extremity for simulating musculoskeletal surgery and analyzing neuromuscular control. *Annals of biomedical engineering*, 33(6), pp.829-840.

Karsai, I., Conceição, A. and Takács, L., 2019. Reliability of the 3D Underwater Motion Analysis. *Motricidade*, 15, pp.104-104.

Katiyar, R., Pathak, D. and Kumar, V., 2010. Clinical gait data analysis based on Spatio-Temporal features. *arXiv preprint arXiv:1003.1511*.

Kirtley, C., 2006. *Clinical gait analysis: theory and practice*. Elsevier Health Sciences.

Krupenevich, R., n.d. Effect of low-pass filter cutoff frequencies on joint moments in walking.

Liu, M.Q., Anderson, F.C., Schwartz, M.H. and Delp, S.L., 2008. Muscle contributions to support and progression over a range of walking speeds. *Journal of biomechanics*, 41(15), pp.3243-3252.

Mirmoezzi, M., Sadeghi, H., Rahimi, A. and Khazaeli, M., 2015. Comparison of Kinematic Characteristics of Body Motion in Free Throws and Jump Shots of Basketball Adult Players.

Moriguchi, C.S., Sato, T.O. and Gil Coury, H.J.C., 2007. Ankle movements during normal gait evaluated by flexible electrogoniometer. *Brazilian Journal of Physical Therapy*, 11(3), pp.205-211.

Musculoskeletal Key, 2016. *Normal gait*. Available through: <<https://musculoskeletalkey.com/normal-gait/>> [Accessed 18 Aug. 2019].

Nandy, A., Bhowmick, S., Chakraborty, P. and Nandi, G.C., 2014. Gait Biometrics: An Approach to Speed Invariant Human Gait Analysis for Person Identification. In *Proceedings of the Second International Conference on Soft Computing for Problem Solving (SocProS 2012), December 28-30, 2012* (pp. 729-737). Springer, New Delhi.

Nemtsev, O.B. and Nemtseva, N.A., 2017. Kinematic Analysis of Resist-and-Release Sprint Running. *ISBS Proceedings Archive*, 35(1), p.271.

Nemtsev, O.B., Nemtseva, N.A., Kozlov, I.S., Doronin, A.M. and Shubin, M.S., 2015. Biomechanical analysis of the best and the worst trials of takeoff in long jump among the combine events athletes.

Nigg, B.M., Fisher, V. and Ronsky, J.L., 1994. Gait characteristics as a function of age and gender. *Gait & posture*, 2(4), pp.213-220.

Nikravesh, P.E., 1988. *Computer-aided analysis of mechanical systems*. Prentice-Hall, Inc..

Noehren, B., Schmitz, A., Hempel, R., Westlake, C. and Black, W., 2014. Assessment of strength, flexibility, and running mechanics in men with iliotibial band syndrome. *Journal of orthopaedic & sports physical therapy*, 44(3), pp.217-222.

Nunes, J.F., Moreira, P.M. and Tavares, J.M.R., 2016. Human motion analysis and simulation tools: a survey. In *Handbook of research on computational simulation and modeling in engineering* (pp. 359-388). IGI Global.

Oberg, T., Karsznia, A. and Oberg, K., 1994. Joint angle parameters in gait: reference data for normal subjects, 10-79 years of age. *Journal of rehabilitation research and development*, 31(3), pp.199-213.

Oliveira, H., 2016. Inverse Dynamic Analysis of the Human Locomotion Apparatus for Gait.

Olney, S.J., Griffin, M.P., Monga, T.N. and McBride, I.D., 1991. Work and power in gait of stroke patients. *Archives of physical medicine and rehabilitation*, 72(5), pp.309-314.

Omorczyk, J., Nosiadek, L., Nosiadek, A. and Chwała, W., 2014. Use of biomechanical analysis for technical training in artistic gymnastics using the example of a back handspring. *Selected problems of biomechins of sports and rehabilitation vol II*.

Pearsall, D.J. and Costigan, P.A., 1999. The effect of segment parameter error on gait analysis results. *Gait & Posture*, 9(3), pp.173-183.

Perry, J. and Davids, J.R., 1992. Gait analysis: normal and pathological function. *Journal of Pediatric Orthopaedics*, 12(6), p.815.

Pfister, A., West, A.M., Bronner, S. and Noah, J.A., 2014. Comparative abilities of Microsoft Kinect and Vicon 3D motion capture for gait analysis. *Journal of medical engineering & technology*, 38(5), pp.274-280.

Prakash, C., Gupta, K., Mittal, A., Kumar, R. and Laxmi, V., 2015. Passive marker based optical system for gait kinematics for lower extremity. *Procedia Computer Science*, 45, pp.176-185.

Qiu, S., Liu, L., Li, J., Wang, Z., Qin, K. and Jiang, Y., 2017, July. Gaitsense: A potential assistance for physical rehabilitation by means of wearable sensors. In *2017 IEEE International Conference on Computational Science and Engineering (CSE) and IEEE International Conference on Embedded and Ubiquitous Computing (EUC)* (Vol. 1, pp. 116-121). IEEE.

Rao, G., Amarantini, D., Berton, E. and Favier, D., 2006. Influence of body segments' parameters estimation models on inverse dynamics solutions during gait. *Journal of biomechanics*, 39(8), pp.1531-1536.

Ren, L., Jones, R.K. and Howard, D., 2005. Dynamic analysis of load carriage biomechanics during level walking. *Journal of biomechanics*, 38(4), pp.853-863.

Ren, L., Jones, R.K. and Howard, D., 2008. Whole body inverse dynamics over a complete gait cycle based only on measured kinematics. *Journal of biomechanics*, 41(12), pp.2750-2759.

Robert, T., Chèze, L., Dumas, R. and Verriest, J.P., 2007. Validation of net joint loads calculated by inverse dynamics in case of complex movements: application to balance recovery movements. *Journal of biomechanics*, 40(11), pp.2450-2456.

Root, M.L., Orien, W.P. and Weed, J.H., 1977 Normal and abnormal function of the foot. *Clinical biomechanics*, 2.

Schache, A.G. and Baker, R., 2007. On the expression of joint moments during gait. *Gait & posture*, 25(3), pp.440-452.

Seth, A., Sherman, M., Reinbolt, J.A. and Delp, S.L., 2011. OpenSim: a musculoskeletal modeling and simulation framework for in silico investigations and exchange. *Procedia Iutam*, 2, pp.212-232.

Siegler, S. and Liu, W., 1997. Inverse dynamics in human locomotion. *Three-dimensional analysis of human locomotion*, pp.191-209.

Siegler, S., Seliktar, R. and Hyman, W., 1982. Simulation of human gait with the aid of a simple mechanical model. *Journal of biomechanics*, 15(6), pp.415-425.

Silva, M.P. and Ambrósio, J.A., 2004. Sensitivity of the results produced by the inverse dynamic analysis of a human stride to perturbed input data. *Gait & posture*, 19(1), pp.35-49.

Silvestre, G., Mataloto, J., Borges, D., Conceição, A., Louro, H. and Branco, M., 2019. Analysis of the human walking gait with and without external weight added on lower limbs of physically active individuals. *Motricidade*, 15, pp.69-69.

Sobhani, S., Dekker, R., Postema, K. and Dijkstra, P.U., 2013. Epidemiology of ankle and foot overuse injuries in sports: a systematic review. *Scandinavian journal of medicine & science in sports*, 23(6), pp.669-686.

Stauffer, R.N., Chao, E.Y. and Brewster, R.C., 1977. Force and motion analysis of the normal, diseased, and prosthetic ankle joint. *Clinical orthopaedics and related research*, (127), pp.189-196.

Thomas, G.W., Johns, B.D., Marsh, J.L. and Anderson, D.D., 2014. A review of the role of simulation in developing and accessing orthopaedic surgical skills. *The Iowa orthopaedic journal*, 34, p.181.

Toda, H., Nagano, A. and Luo, Z., 2015. Age and gender differences in the control of vertical ground reaction force by the hip, knee and ankle joints. *Journal of physical therapy science*, 27(6), pp.1833-1838.

Ugbolue, U.C., Papi, E., Kaliarntas, K.T., Kerr, A., Earl, L., Pomeroy, V.M. and Rowe, P.J., 2013. The evaluation of an inexpensive, 2D, video based gait assessment system for clinical use. *Gait & posture*, 38(3), pp.483-489.

Umberger, B.R. and Martin, P.E., 2001. Testing the planar assumption during ergometer cycling. *Journal of Applied Biomechanics*, 17(1), pp.55-62.

Vaughan, C.L., Davis, B.L. and O'connor, J.C., 1992. *Dynamics of human gait* (Vol. 2). Human Kinetics.

Watkins, J., 2010. Structure and function of the foot. *Neale's Disorders of the Foot*, p.387.

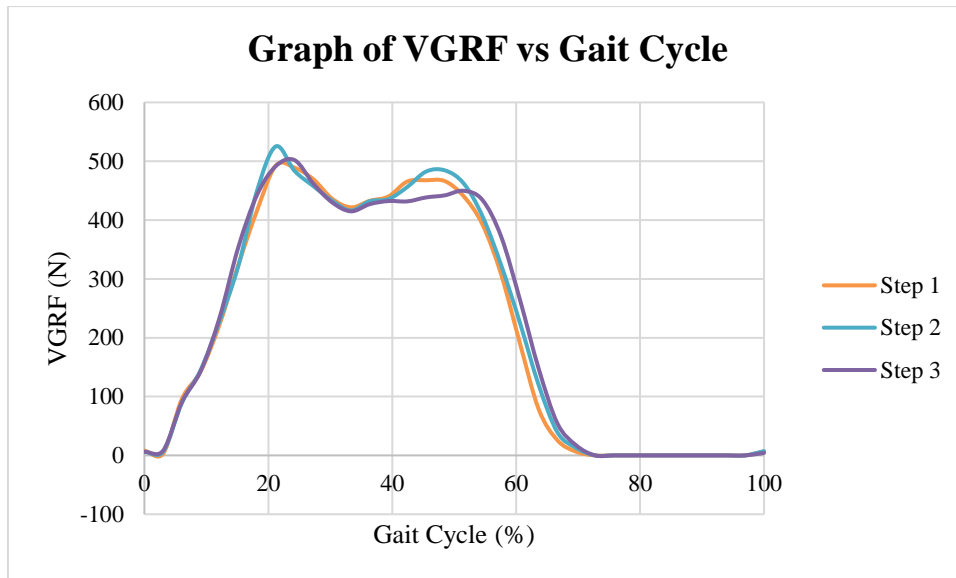
Winter, D.A., 1987. *The biomechanics and motor control of human gait*. Waterloo.

Winter, D.A., 2009. *Biomechanics and motor control of human movement*. John Wiley & Sons.

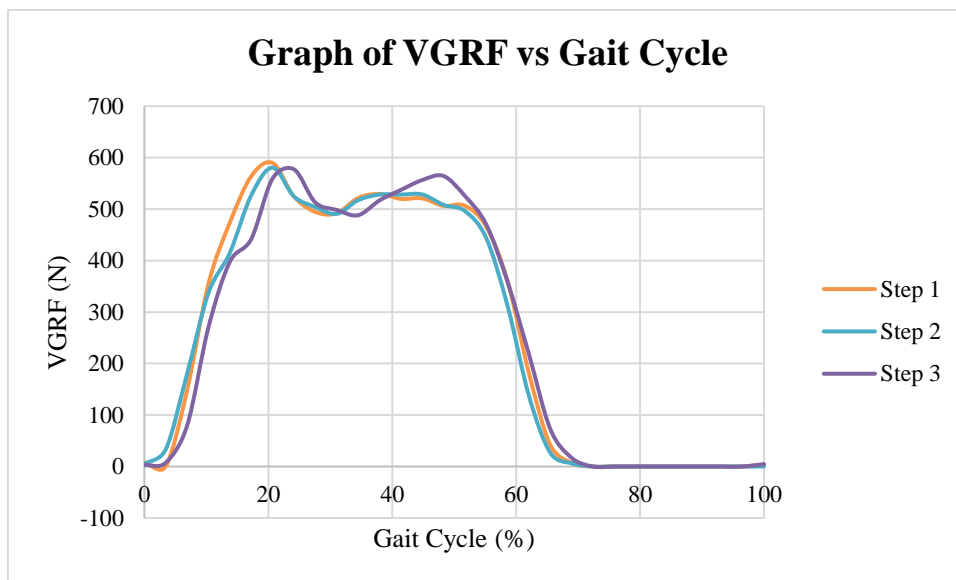
Winter, D.A., Quanbury, A.O., Hobson, D.A., Sidwall, H.G., Reimer, G., Trenholm, B.G., Steinke, T. and Shlosser, H., 1974. Kinematics of normal locomotion—a statistical study based on TV data. *Journal of Biomechanics*, 7(6), pp.479-486.

APPENDICES

APPENDIX A: Graphs



Graph A-1: The Graph of VGRF against Gait Cycle for Female Subject.



Graph A-2: The Graph of VGRF against Gait Cycle for Male Subject.